2021•2022

Faculteit Industriële Ingenieurswetenschappen

master in de industriële wetenschappen: chemie

Masterthesis

Kinetic study of the degradation of sulfamethoxazole by uv light combined with H2O2 and photo-fenton treatment

PROMOTOR :

Prof. dr. ir. Leen THOMASSEN

PROMOTOR :

Prof. dr. ir. Natalia VILLOTA

BEGELEIDER :

Prof. dr. Jeroen LIEVENS

BEGELEIDER :

Prof. dr. Jose Maria LOMAS

Sebastien Jankelevitch

Scriptie ingediend tot het behalen van de graad van master in de industriële wetenschappen: chemie

Gezamenlijke opleiding UHasselt en KU Leuven

2021•2022

Faculteit Industriële Ingenieurswetenschappen

master in de industriële wetenschappen: chemie

Masterthesis

Kinetic study of the degradation of sulfamethoxazole by uv light combined with H2O2 and photo-fenton treatment

PROMOTOR :

Prof. dr. ir. Leen THOMASSEN

PROMOTOR :

Prof. dr. ir. Natalia VILLOTA

BEGELEIDER :

Prof. dr. Jeroen LIEVENS

BEGELEIDER :

Prof. dr. Jose Maria LOMAS

Sebastien Jankelevitch

Scriptie ingediend tot het behalen van de graad van master in de industriële wetenschappen: chemie

UHASSELT KU LEUVEN

PREFACE

This master's thesis was written on an Erasmus+ exchange programme. From the small town of Hasselt I have travelled to Vitoria-Gasteiz in Spain to work together with the faculty of Industrial Engineering of the University of the Basque Country. I was warmly welcomed by professor Villota and professor Lomas, who have both greatly helped me acclimate to my stay. First and foremost I would like to thank them for their patience and time spent guiding me during the thesis work.

Secondly, I want to thank the faculty of Chemical Engineering Technology at UHasselt and KULeuven for making this experience possible. An Erasmus+ exchange has its challenges, but rewards the student with a new perspective on life, culture and people. To connect this with the lessons you learn from entering a new professional environment in a different language makes for valuable growth in one's character. I would like to especially thank professor Leen Thomassen for her guidance during the thesis work and Greet Raymaekers for time spent arranging the exchange.

The thesis work encompasses an unorthodox way for the analysis of the degradation of an antibiotic (sulfamethoxazole), which I am excited to share with you.

CONTENTS

LIST OF TABLES

LIST OF FIGURES

GLOSSARY

AOP = Advanced oxidation process
CEC = Contaminant of emerging concern
CP = chlorinated parrafin
EQSD = Environmental quality standards directive
EQS = Environmental quality standard = maximal concentration allowed in the environment
AA-EQS = Average annual EQS = maximal annual average concentration allowed in the environment
SMX = Sulfamethoxazole
WFD = Water framework directive
WWTP = Waste water treatment plant

ABSTRACT IN ENGLISH

Sulfamethoxazole is an orally ingested sulfonamide antibiotic. It makes its way to water treatment plants through human waste and sewage. Sulfamethoxazole (SMX) is not efficiently degraded by the biological treatment of modern water treatment plants due to its bacteriostatic effect. Furthermore, the effect of continuous exposure to sulfamethoxazole on the aquatic environment and human health is unknown. This thesis aims to increase the current knowledge about sulfamethoxazole degradation by proposing a degradation pathway and by kinetically modelling physical and chemical parameters (color, turbidity, aromaticity) during the degradation.

The tests were conducted by oxidizing aqueous solutions of SMX 50.0 mg L^{-1} of 1.0 L in a photocatalytic reactor that used a 150 W UV mercury lamp and 100.0 mM hydrogen peroxide. The temperature was maintained around 25ºC. Assays were performed under different pH conditions (pH between 2.0 and 12.0), and the pH was kept constant during the treatment by adding diluted NaOH and HCl. Further testing was also done with Fe^{2+} catalyst, with varying dose of catalyst, H_2O_2 and pH. IC analysis and measurement of physical and chemical parameters was done on a sample taken every 5 minutes during the reactions.

In conclusion, the effect of pH was attributed to the ionization of SMX. Also, a pseudo first-order model (UV/H_2O_2) and second-order model (photo-Fenton) was set up to model kinetics of the degradation. These findings are in line with existing literature of this degradation.

ABSTRACT IN DUTCH

Sulfamethoxazol (SMX) is een sulfonamide antibioticum dat oraal wordt toegediend. Via het rioleringssysteem komt het na excretie terecht in afvalwaterzuiveringsinstallaties. De biologische zuivering van de moderne zuiveringsinstallaties verwijdert het SMX niet efficiënt door het bacteriostatisch effect van het antibioticum. Ook is het effect van langdurige blootstelling aan SMX op het aquatisch milieu en op de menselijke gezondheid niet bekend. Deze thesis beschrijft de degradatie van SMX door een degradatie schema voor te stellen en fysische en chemische parameters (kleur, troebelheid, aromaticiteit) kinetisch te modelleren.

Een 1.0 L oplossing van 50 mg L^{-1} SMX reageerde met 100 mM H_2O_2 in een fotokatalytische reactor met een 150W kwik UV lamp. De temperatuur was constant op 25°C. De pH varieerde tijdens verschillende testen tussen 2.0 en 12.0 en bleef constant tijdens de reactie door het toevoegen van 0.1 M NaOH en HCl. In verdere testen bevatte de oplossing ook Fe^{2+} als katalysator en het effect van de hoeveelheid katalysator, de concentratie H_2O_2 en pH op de kinetiek werd onderzocht. De stalen werden geanalyseerd met behulp van ionchromatografie en meting van de fysische en chemische parameters.

Het effect van pH op het degradatie schema werd toegewezen aan de ionizatie van het SMX. Om de parameters van de UV/H_2O_2 reactie te beschrijven werd een pseudo-eerste orde model gebruikt, terwijl voor de foto-Fenton reactie een tweede orde model werd opgesteld. Deze bevindingen zijn in lijn met de resultaten in de literatuur.

1. INTRODUCTION

1.1. ENVIRONMENTAL CURRENT ISSUES ABOUT WATER AND CONTAMINANTS OF EMERGING CONCERN

The health of our aquatic ecosystems is important for our society. Water is a common good on which life depends. The EU has released multiple directives throughout history pertaining the safety of its water resources. In 2012 they released the Blueprint to Safeguard Europe's Water Resources, which is the most recent long-term strategy with the goal of ensuring the availability of water of sufficient quality for all legitimate uses. In this blueprint, the pressure on our aquatic ecosystems is attributed to the following causes: pollutant emissions, water over-use (water stress), physical changes to water bodies (i.e. erosion, thermal conditions…) and extreme events such as floods and drought (European Union, 2012). The legal framework for this blueprint dates back to the EU water framework directive (2000/60/EC) or WFD in short. The WFD aims to achieve good environmental status for inland surface waters, transitional waters, coastal waters and groundwater. The framework is supported by more specific directives such as: the Groundwater Directive (2006/118/EC), the Drinking Water Directive (EU 2020/2184), the Bathing Water Directive (2006/7/EC), the Nitrates Directive (91/676/EEC), the Urban Waste Water Treatment Directive (91/271/EEC), the Environmental Quality Standards Directive (EQSD) (2008/105/EC) and the Floods Directive (2007/60/EC) (Kurrer, 2021). In the Environmental Quality Standards Directive a concentration limit is imposed on 33 priority substances, which present a risk to or via the aquatic environment. This list is supplemented by control of 8 other substances only in surface waters and a watch-list of substances which are constantly reviewed to be priority substances. Strictly speaking, the compounds on the watch-list are the ones that best fit the definition of emerging pollutants, considering that they are pollutants whose degree of presence, concentration or impact on the aquatic environment are unknown. They are contaminants about which there are suspicions that they may pose a significant risk, but about which there is little information nor specific regulation. This list must be updated by the Commission every two years. The established strategy involves deepening the knowledge of these substances, their presence and effects. It is important to note that all threshold values of pollutants, except for nitrates and pesticides, are set by the Member states (European Union, 2008).

To comply with all these directives, industrial and sewage effluents are cleaned in wastewater treatment plants (WWTPs) . This usually happens with a primary physical treatment, followed by a biological secondary treatment and tertiary physical or chemical treatment depending on the contaminants in the influent and the wanted specifications of the effluent (Moran, 2018). The tertiary treatment focusses on cleaning the effluent of remaining pollutants so that it can be released according to local legislation. In the present day, increasing analytical capability makes way for detecting the presence of pollutants in natural effluents at lower concentrations. In many cases, the effect of these emerging pollutants on the health of living beings or the health of the aquatic ecosystem is not known (Kuster et al., 2008; Petrovic et al., 2009). The contaminants of emerging concern

(CECs) may initially present low acute toxicity, but can manifest health risks in different ways such as disrupting hormonal function in the body or they can degrade to more hazardous substances (United Stated Environmental Protection Agency (EPA), n.d.).

1.2. CONTAMINANTS OF EMERGING CONCERN CLASSIFICATION

As mentioned above CECs have three common characteristics: they are presently found in water bodies, pose potential health risks for humans or the environment and are often not regulated under current legislation. Examples of CECs and their health risks are now listed.

1.2.1. Flame retardants

Flame retardants are chemicals added to materials to make them less flammable. The most commonly used flame retardants are brominated flame retardants, such as polybrominated diphenyl ether as shown in figure 1:

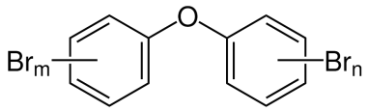

Figure 1: Polybrominated diphenyl ether

These flame retardants are persistent molecules and for this reason, have been shown to accumulate in the environment as well as living beings (=bioaccumulate) (Oberg & Warman, 2002; Watanabe, 1987). They have been proven to affect human health in the form of thyroid hormone homeostasis and chronic neurotoxicity (Alaee & Wenning, 2002; Kim et al., 2014). It has to be noted that brominated diphenyl ethers are regulated by the EQSD to a concentration of 0,5 ng/l in surface water. This concentration is called an environmental quality standard (EQS) is applied on 6 specific brominated diphenyl ethers. The concentrations are counted separately unless mentioned otherwise and are targeted at the concentration of these compounds in surface water. Both annual average (AA-EQS) and maximal allowed concentration (MAC-EQS) is defined in the EQSD but in this literature study only annual average is listed.

1.2.2. Chlorinated paraffins

Chlorinated paraffins (CPs) are paraffins of varying length, branched with a varying number of chlorine groups. They are commonly used as plasticizer for PVC, but can also have use as a water-repellent or flame retardant in materials. The CPs are divided into three groups: short-chain CPs (SCCPs), medium-chain CPs (MCCPs) and long-chain CPs (LCCPs) (Rossberg et al., 2006). An example of a medium-chain chlorinated paraffin is shown in Figure 2:

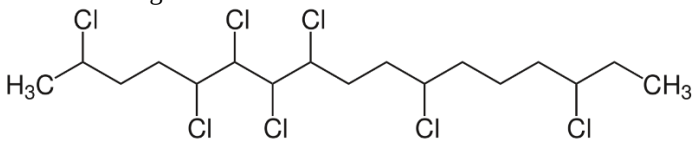

Figure 2: Example of a medium-chain chlorinated paraffin

CPs are shown to be persistent molecules and thus bioaccumulate similarly to flame retardants. SCCPs (C10-C13) are already regulated by the EQSD (0,4 µg/l), but MCCPs and LCCPs are not. There is a growing concern regarding MCCPs due to their toxicity to the aquatic environment (Glüge et al., 2018). For this reason, some MCCPs are under review in the EQSD.

1.2.3. Fertilizers and pesticides

Fertilizers and pesticides are used to increase the efficiency of our food production industry. Fertilizers provide nutrients for the growth of crops, while pesticides defend crops from pests. They are important for the production of food on farmlands, but water from extreme rainfall and irrigation can cause the fertilizers and pesticides to flow into groundwater and freshwater supplies. Many organic pesticides such as atrazine (0,6 μg/l) and cyclodiene pesticides (sum cannot exceed 0,01 μg/l) are already regulated in the EQSD due to growing concerns regarding their health effects (Jaeger et al., 1999; Younes & Galal-Gorchev, 2000). Meanwhile, only one inorganic pesticide, glyphosate, is mentioned in the EQSD and as of now is still under review. Public opinion dictates that inorganic/natural pesticides are better than organic/synthetic ones, but some caution is needed regarding inorganic pesticides (Bahlai et al., 2010). Fertilizers are found to be less persistent and less toxic to the environment and are thus regulated at a higher EQS. Nitrates for example have an AA-EQS of 50 mg/l in the nitrates directive.

1.2.4. Perfluorinated compounds

Perfluorinated compounds (PFCs) contain no C-H bonds. Every carbon is mostly bonded with fluorine groups. PFCs are characterised by the bonds with other heteroatoms. PFCs have been extensively used in industrial, commercial and consumer applications. An example of this is Perfluorooctanesulfonic acid (PFOS), shown in Figure 3, is used in fabric protectors such as Scotchgard produced by 3M. PFOS functions as a stain and water repellent (Sherman & Smith, 1971). PFOS is also on the review list in the EQSD.

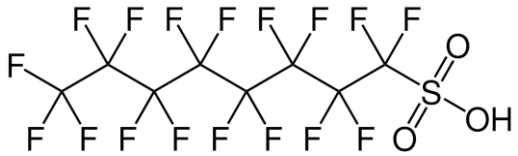

Figure 3: Perfluorooctanesulfonic acid

Use of many PFCs is under scrutiny due to their toxicity to human health and environment, but data on the health effects of many PFCs is sparse (Steenland et al., 2010). PFCs are very persistent molecules. Traces have been found in children (Y. Zhang et al., 2022), human milk (Rawn et al., 2022) and even fish embryos (X. Wang et al., 2022).

1.2.5. Pharmaceutical products

More pharmaceutical products find their way into the environment as a result of increased use, an increase in population and population aging (Dieleman et al., 2017; Tev et al., 2011). The pharmaceutical and personal care products (PCCPs) are disposed through excretion and household waste. Incomplete removal of PCCPs in wastewater treatment can cause health risks, but their long term health risks remain poorly understood (Halling-Sorensen et al., 1998; Kmmerer, 2010). PCCPs encompass a wide group of chemicals, of which some subgroups are now further looked at.

1.2.5.1. Analgesics

Analgesics are more commonly referred to as painkillers. Of this subgroup, paracetamol stands out, because it is one of the most widely detected drugs in freshwater environments with higher concentrations of 6-65 μg/l (Murray et al., 2010). Paracetamol is shown in Figure 4:

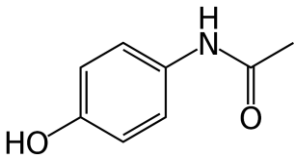

Figure 4: Structure of paracetamol

1.2.5.2. Antidepressants

A common treatment for major depressive disorder or anxiety disorders are antidepressants. Antidepressants inhibit the reuptake of neurotransmitters serotonin, dopamine and norepinephrine (Z. Zhou et al., 2007). They can cause imbalance in natural neurotransmitter levels in organisms through indirect exposure (Fent et al., 2006). They also can cause side effects in humans, which include weight gain and sexual dysfunction. Figure 5 shows the structure of venlafaxine, a serotonin-noradrenaline reuptake inhibitor (SNRI).

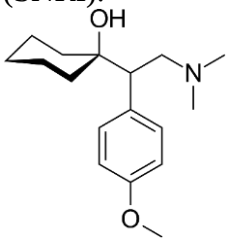

Figure 5: Venlaxafine

1.2.5.3. Antibiotics

Antibiotics are used to fight bacterial infections. It is believed that the discharge of antibiotics in the aquatic environment may favor the growth of persistent bacteria (Petrović et al., 2003). Examples of antibiotics include penicillin and sulfamethoxazole.

A better understanding of these compounds and their degradation is needed to determine their effect on the aquatic environment and their threat to humans. For this reason the Engineering faculty of Vitoria-Gasteiz at the University of the Basque Country has selected some of these CECs to be studied. Their degradation kinetics and intermediates will be determined. This list of CECs includes caffeine, paracetamol, sulfamethoxazole and others.

1.3. SULFAMETHOXAZOLE

This study focusses on the degradation of sulfamethoxazole (SMX) and its kinetics. A better understanding of the degradation of SMX is paramount for the estimation of the environmental impact of SMX in the aquatic environment. Its structure is shown in Figure 6:

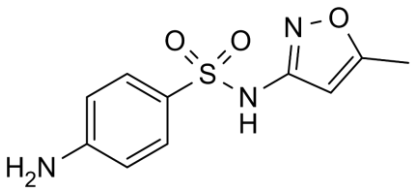

Figure 6: Structure of sulfamethoxazole

Sulfamethoxazole is an antibiotic commonly used in combination with trimethoprim (TMP). This combination is described by WHO as the optimal treatment for urinary tract infections (Roth et al., 2018).

1.3.1. Effect and toxicity on humans

Sulfamethoxazole is an orally ingested antibiotic and it inhibits dihydropteroate synthase. It arrives in the bloodstream by travelling through the gastrointestinal tract. Dihydropteroate synthase is responsible for conversion of para-aminobenzoic acid to folic acid. Bacteria need folic acid for growth and division. Removing the ability of the bacteria to grow is called a bacteriostatic effect (FDA, n.d.). The immune system disposes of the bacteria on its own pace after SMX has removed their ability to grow. SMX is used for battling bacterial infections for these reasons, but it also has adverse side effects. Common side effects include nausea, vomiting and loss of appetite (FDA, n.d.). It can also cause problems for people allergic to sulphonamides. Common allergic reactions are: skin rashes, eosinophilia and drug fever. Very dangerous reactions are uncommon (Choquet-Kastylevsky et al., 2002).

1.3.2. Environmental issues

Sulfamethoxazole can have a significant effect on the environment due to its bacteriostatic effect. It could potentially stop enriching bacteria from growing and thus remove the balance of an aquatic ecosystem (C. Underwood et al., 2011). Information about long term effects of SMX or SMX degradation in the environment is sparse.

1.4. EMERGING CONTAMINANTS IN RESIDUAL WATERS

An estimation of the number of pharmaceuticals in the aquatic environment is shown in Figure 7 (der Beek et al., 2015, p.829):

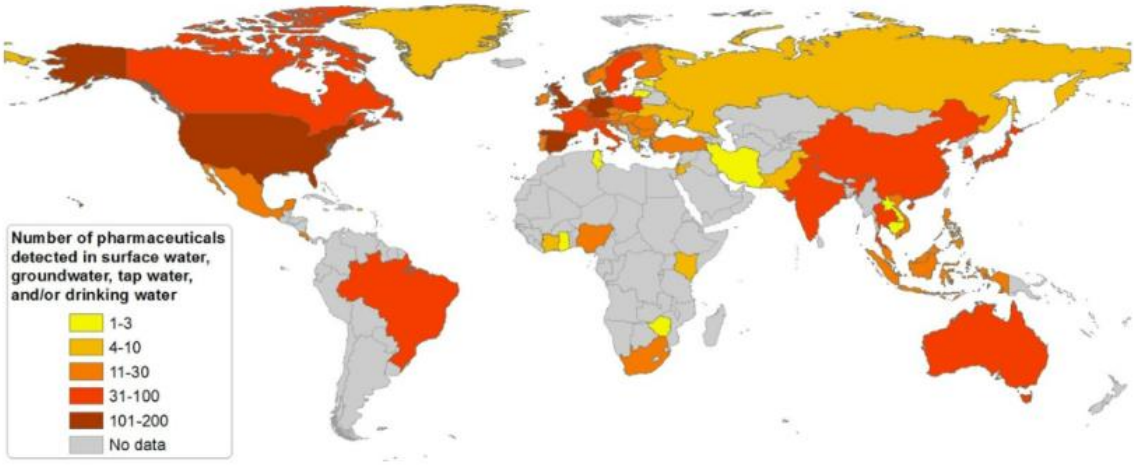

Figure 7: Number of pharmaceutical substances detected in surface waters, groundwater, or tap/drinking water (der Beek et al., 2015, p.829).

A big source of pharmaceuticals is human waste, which passes through the wastewater treatment plants. WWTPs are not designed to treat this type of compound. For this reason, the CECs are not completely degraded, and in the end they are discharged into natural channels through the outlet water and sludge (Diniz et al., 2010). Therefore, a high percentage of them and their metabolites pass into the aquatic environment. It is not necessary for this group of pollutants to persist in the environment to cause negative

effects, since their elimination or transformation can be compensated by their continuous introduction into the environment (Daughton, 2004). For this reason, the development of efficient methods for the elimination of these contaminants is essential to avoid environmental contamination and the potential damage that these compounds can exert on living beings.

Sulfamethoxazole can be present in surface water in the range of nanogram per litre to microgram per litre (Gao et al., 2016; J. Wang & Wang, 2016). The removal of SMX in WWTPs is different depending on different treatment steps in the plant as well as the microorganisms used. The microbial effect can be shown by examining the SMX removal capacity of two different WWTPs with only a biological treatment. Rosal et al. and Zhou et al. both find different removal capacity's in their studied biological treatment (Rosal et al., 2010; L. J. Zhou et al., 2013). Rosal et al. find a removal capacity of below 20%, while Zhou et al. report a removal capacity of 40% for an oxidation ditch and 70% for a cyclic activated sludge system. A review of multiple studies regarding WWTP effluents over the world concludes that biological treatments with an AOP as an added step leads to more removal capacity of SMX (J. Wang & Wang, 2018).

1.5. ADVANCED OXIDATION PROCESSES

In recent years, advanced oxidation processes (AOPs) have been studied to remove organic compounds from water. AOPs, such as Fenton oxidation, are defined by their creation of reactive hydroxyl radicals from an oxidant (H_2O_2, O_3…) with a catalyst (UV-light, ultrasonic waves, metal salts or semiconductors). The Fenton process is a viable method for elimination of organic contaminants present in wastewater and is already applied in industry. However, the produced metal sludge from the iron catalyst has to be properly managed due to the strict directives from the European Union regarding iron in effluents (200 µg/l max. in drinking water). The goal of a Fenton process is production of hydroxyl radicals to decompose organic pollutants with these radicals as illustrated with the following formulas (Braeken, 2021) (Pera-Titus et al., 2004):

Initiation:

$$H_2O_2 + Fe^{2+} \rightarrow Fe^{3+} + OH^- + HO\cdot$$
$$H_2O_2 + Fe^{3+} \rightarrow Fe(OOH)^{2+} + H^+ \leftrightarrows Fe^{2+} + HO_2\cdot + H^+$$
$$OH^- + Fe^{3+} \rightarrow Fe(OH)^{2+} \leftrightarrows Fe^{2+} + HO\cdot$$

Propagation:

$$HO\cdot + H_2O_2 \rightarrow HO_2\cdot + H_2O$$
$$HO_2\cdot + H_2O_2 \rightarrow HO\cdot + H_2O + O_2$$
$$HO_2\cdot + {HO_2}^- \rightarrow HO\cdot + OH^- + O_2$$

Termination:

$$Fe^{2+} + HO\cdot \rightarrow Fe^{3+} + OH^- \qquad HO_2\cdot + Fe^{3+} \rightarrow Fe^{2+} + H^+ + O_2$$
$$HO\cdot + HO_2\cdot \rightarrow H_2O + O_2 \qquad HO\cdot + HO\cdot \rightarrow H_2O_2$$
$$Pollutant + HO\cdot \rightarrow Intermediates$$
$$Intermediates + HO\cdot \rightarrow CO_2 + H_2O + anorganic\ salts$$

1.5.1. Hydroxyl radical

In water treatment, hydroxyl radicals are usually produced by the degradation of peroxides. They have a standard oxidation potential of 2,8V, while O_3 has 2,07V and H_2O_2 has 1,78V. This increased reactivity makes them a good choice for oxidation of pollutants (Pera-Titus et al., 2004). Hydroxyl radicals react with organic molecules very quickly, as their rates approach diffusion-limited characteristics (10^9–10^{10} M^{-1} s^{-1})

(Kehrer et al., 2010). The radicals are not selective because of their high reactivity and can react with water or other radicals with lower reactivity if no organic material is close to the site of formation. Unwanted molecules that react easily with the hydroxyl radicals are called scavengers, an example of this is Cl^-. For this reason, a Fenton process will be less efficient in saline water (Buxton et al., 2009).

1.5.2. Advanced photochemical oxidation processes

1.5.2.1. UV Radiation

UV radiation is electromagnetic radiation with a wavelength between 10 nm and 400 nm. UV radiation can be used as a catalyst as it introduces more energy into the system. This energy can be used to break chemical bonds or to cause ionization. UV photolysis has been used to remove pollutants directly (Boule et al., 1984; Legrini et al., 2002), but is more effective when combined with hydrogen peroxide or ozone. The UV-light can then create hydroxyl radicals, which cause oxidative degradation of pollutants instead of photolysis.

1.5.2.2. Photo-Fenton Treatment

With the addition of energy from UV-light to a Fenton process, a photo-Fenton process is created. This has two important benefits: increased production of hydroxyl radicals and decreased amount of metal sludge due to regeneration of the iron catalyst. This is illustrated in the following reactions (Pera-Titus et al., 2004):

Photolysis to create more radicals: $H_2O_2 + hv \rightarrow 2OH\cdot$

Regeneration of iron catalyst: $Fe^{3+} + OH^- \rightarrow Fe(OH)^{2+}$

$Fe(OH)^{2+} + hv \rightarrow Fe^{2+} + OH\cdot$

The degree of oxidation achieved with these technologies depends both on the reduction of Fe^{3+} to Fe^{2+} that regenerates the catalyst, as well as on the pH, the concentration of catalyst, hydrogen peroxide and temperature. Pera-Titus et al. also describe trends regarding the process parameters. They state that the optimal process pH is between 2 and 4. Decomposition of pollutant significantly decreases if pH increases above 4, due to the formation of iron hydroxide precipitation. Increase in concentration of iron catalyst increases the decomposition of the pollutant, but this increase gradually slows down at higher concentrations of catalyst. Increasing the concentration of H_2O_2 also increases the decomposition. Other studies confirm these findings (Chamarro et al., 2001; Pandis et al., 2022). The ratio of H_2O_2 to iron is important. The optimal ratio is believed to be 1 part of iron to between 5 and 25 parts of H_2O_2 for ozonisation of chlorophenols (Pera-Titus et al., 2004; Walling, 2002). It is believed that higher values of this ratio support the termination reactions. For sulfamethoxazole decomposition the ratio of catalyst to H_2O_2 may be different than for chlorophenols. Trovo et al. increased the ratio up to 1 part iron and 20 parts H_2O_2, which was the optimal run for these tests regarding decomposition of sulfamethoxazole (Trovó et al., 2009).

1.6. SULFAMETHOXAZOLE DEGRADATION PATHWAY

Some research has been done regarding the degradation pathway of sulfamethoxazole. The degradation of sulfamethoxazole through oxidative processes is found to happen through 3 major pathways. Firstly, a pathway is possible where hydroxylation of the rings

occur. In a second pathway the benzene and isoxazole rings are attacked and opened. Thirdly, bond cleavage is possible which is followed by hydrolysis. Figure 8 shows a proposed pathway when the S-N bond of SMX is cleaved. The scheme is a combination of the results found by Gonçalves et al. and Zhong et al. (Gonçalves et al., 2012; Zhong et al., 2021). The left part of the scheme proposes a pathway initiated by the cleavage of the C-N bond next to the S-N bond. This was proposed by Xiong et al. (Xiong et al., 2020):

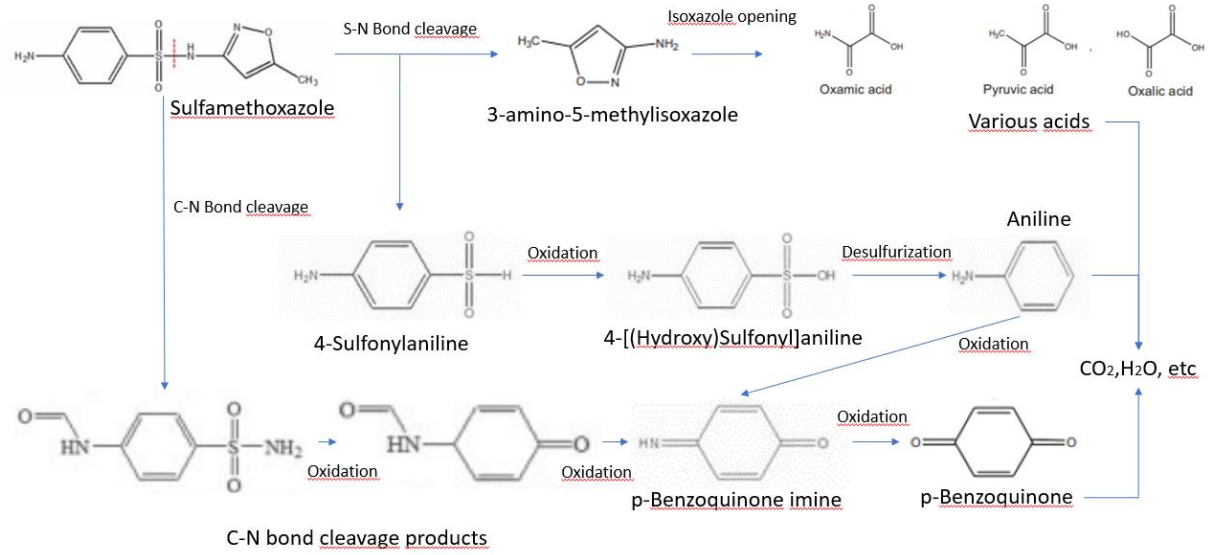

Figure 8: Degradation pathway of SMX during bond cleavage

The other two pathways (hydroxylation and opening of the rings) focus on the attack on the rings without cleavage of bonds in the middle of sulfamethoxazole. Many of the higher masses found in spectroscopy results are a result of these pathways. Trovo et al., Hu et al. and Kumar et al. propose similar pathways in which hydroxylation and opening of the rings takes precedence over bond cleavage (Hu et al., 2007; Kumar et al., 2021; Trovó et al., 2009). Figure 9 shows the scheme presented in Kumar et al., where bond cleavage of the central bonds occurs later in the degradation pathway or, for the right and left pathway, doesn't occur at all.

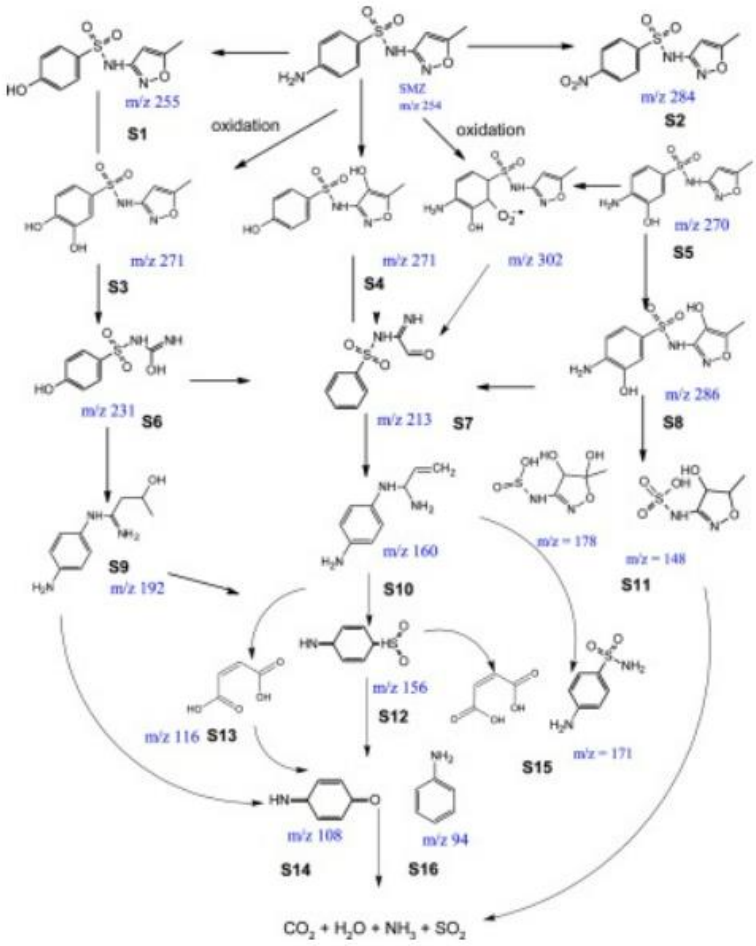

Figure 9: Degradation pathway starting with hydroxylation of the rings and ring opening reactions (Kumar et al., 2021, p.10)

1.7. OBJECTIVES

The objective of this thesis is analysis of the degradation of sulfamethoxazole. A lot of studies have been done regarding the removal capacity of different techniques regarding sulfamethoxazole, but relatively little is known about the exact degradation steps of the compounds. This study aims to create a better understanding of the sulfamethoxazole degradation pathway through finding degradation intermediates and the degradation kinetics. Further research and discussion can indicate whether the proposed compounds are a threat to humans or the environment.

2. MATERIALS AND METHODS

2.1. REACTION SYSTEM

The oxidation tests were conducted with aqueous solutions of sulfamethoxazole $[SMX]_0$=50.0 mg L^{-1} (Fragon, 100,6%) of 1.0 L in a photocatalytic reactor, using a 150 W UV mercury lamp of medium pressure (Heraeus, 85.8 V, 148.8 W, 1.79 A, with 95% transmission between 300 and 570 nm), combined with hydrogen peroxide (Panreac, 30% w/v). The temperature was maintained at (25 ± 5)ºC by means of a cryo-thermostatic bath (Frigiterm- 10 Selecta). Assays were performed operating under different initial pH conditions (pH_0 between 2.0 and 12.0), in order to assess the effect of this parameter on color and turbidity formation during the oxidation of SMX aqueous solutions. Acidity was kept constant by adding NaOH and HCl of 0.1M, as the pH dropped during the reactions due to the formation of acids shown in 1.6. Photo-Fenton reactions were also conducted by adding varying amounts of Fe^{2+}. A solution of 5000 ppm Fe^{2+} was made from $FeSO_4.7H_2O$ (Panreac, 99,0%).

2.2. PHYSICAL/CHEMICAL PARAMETERS AND ANALYSIS METHODS

2.2.1. Ionic chromatography

To measure various acids theorised to be in the degradation pathway a Dionex ICS-5000+ ion chromatograph was used. The specifications of the column are given in Table 1:

Table 1: Ionic chromatograph specifications

Column	Guard: Dionex Ion Pac AG 11-HC-4 μm Analytical: Dionex Ion Pac AG 11-HC-4 μm
Eluent	KOH gradient up to 60 mM, generated by Dionex EGC 500 KOH Eluent Generator Cartridge with Dionex CR-ATC 500 continuously regenerated Anion Trap column
Flow	0.3 ml/min
Injection volume	6,5 μl
Detection	Conductivity with Dionex AERS 500 2mm, 66 mA on external water mode
Run time	48 minutes

Eleven compounds were quantitatively tested: quinate, acetate, pyruvate, succinate, malate, malonate, maleate, oxalate, chloride, nitrate and sulfate. Multielement standards were prepared from concentrations of 2000 ppm of the analytes. The range of concentrations was from 0.5 to 50 ppm for the analytes quinate, acetate, pyruvate, succinate, malate, malonate, maleate and oxalate. Calibration for chloride, nitrate and sulfate was performed in the range of 1 to 100 ppm. The chromatogram for these standard is shown in Figure 10:

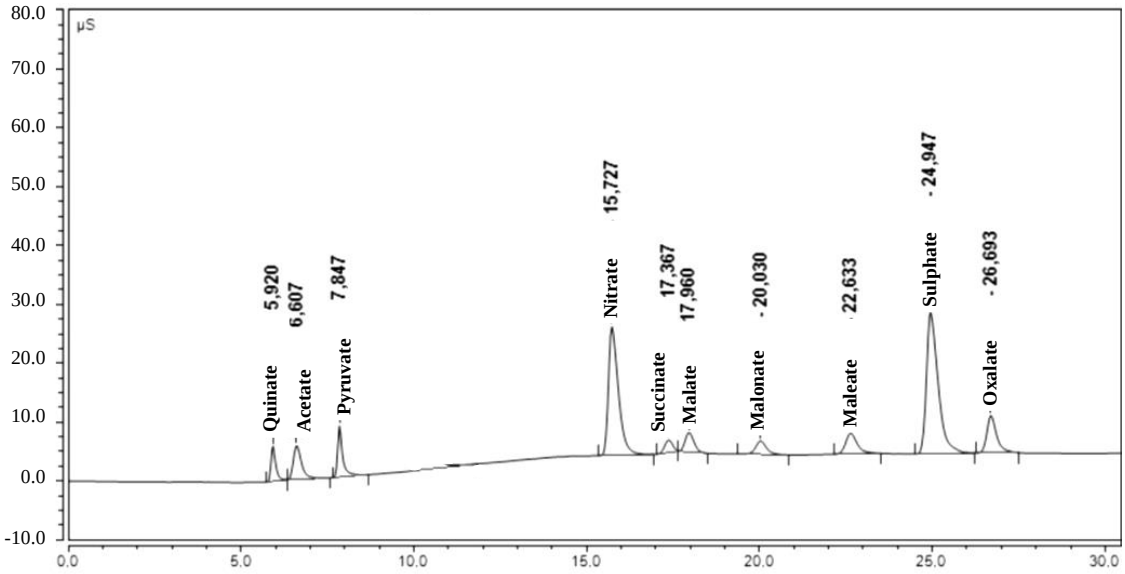

Figure 10: Ionic chromatogram of standards analyzed by Ionic Chromatography

2.2.2. Absorbance at 455 nm (Color)

Color expressed in Absorbance Units (AU) was quantified by the absorbance of the aqueous solution analysed at $\lambda = 455$ nm using a UV/Vis Spectrophotometer 930-Uvikon. This was done following Baird & Bridgewater's spectrophotometric method for color measurement in waste waters (Baird & Bridgewater, 2017). The absorbance of 455 nm was determined to be optimal for the color analysis of similar organic compounds such as paracetamol and phenol (Mijangos et al., 2006; Villota et al., 2016).

2.2.3. Absorbance at 260 nm (SMX degradation)

The sulfamethoxazole degradation is measured at an absorbance of 260 nm. Preferably this would be preceded by a HPLC separation, but the method used in the Industrial Engineering faculty of Vitoria-Gasteiz for analysis of antibiotics did not provide a clear signal for sulfamethoxazole, probably caused by the poor solubility of sulfamethoxazole in water. It was instead decided to measure the absorbance at 260 nm in a JASCO V-730 spectrophotometer as maximum absorbance was measured at this wavelength for a 50 mg/l SMX sample. Aromatic compounds can cause interferrence of the signal, so a critical mindset is needed when examining the results.

2.2.4. Absorbance at 254 nm (Aromaticity)

Aromacity was quantified at $\lambda = 254$ nm using a JASCO V-730 spectrophotometer. The specific ultraviolet absorbance is strongly correlated with the percent aromaticity of the solution (Weishaar et al., 2003).

2.2.5. Turbidity

Turbidity expressed in Nephelometric Turbidity Units (NTU) was measured in a Hach 2100 Turbidimeter. This turbidimeter follows the standard nephelometric method, which

specifies the use of a tungsten filament lamp (Baird & Bridgewater, 2017). Nethelometric turbidity measurement is based on the comparison between intensity of light scattered by a sample and the intensity of the light scattered by a reference. A photoelectric detector measures the light at an angle of 90°.

2.2.6. pH monitoring

Kent EIL 9142 pH meter was used to measure the pH during the course of the reaction.

2.2.7. Temperature monitoring

The UV lamp heats up the solution, for this reason it is important to cool the reactor during experiments. A cooling system (Frigiterm- 10 Selecta) is used that circulates cold water through an outer layer of the UV lamp. During a reaction of 2 hours the temperature can be kept constant at 25°C ± 5°C.

2.2.8. Dissolved oxygen

Dissolved oxygen (DO, mg/L) was measured by a DO-meter HI9142. The electrode is attached to the reactor similarly to the pH electrode.

2.3. PERFORMED REACTIONS

The performed reactions, visible in Table 2, are done by varying one reaction parameter to analyze the effect on the degradation kinetics as well as the effect on formed intermediates. Reaction 1-6 are UV/H_2O_2 reactions, as no Fe^{2+} catalyst is added. In these first 6 reactions the pH is varied between 2 and 12. Following this, 8 reactions are done with Fe^{2+} as catalyst. First, the H_2O_2 concentration was varied from 5 mg/l to 100 mg/l in reactions 7-11. Then, the catalyst concentration was varied from 0.5 mg/l to 5 mg/l in reactions 12-14.

Table 2: Performed sulfamethoxazole degradation reactions

Reaction number	C_0 sulfamethoxazole [mg/l]	C_0 H_2O_2 [mM]	pH	C_0 Fe^{2+} [mg/l]
1	50	100	2	0
2			3	
3			4	
4			6	
5			9	
6			12	
7		100	3	2
8		50		
9		25		
10		10		
11		5		
12		10		0.5
13				1
14				5

3. RESULTS AND DISCUSSION

3.1. UV/H_2O_2 reactions with varying pH

3.1.1. Sulfamethoxazole degradation

As mentioned in 2.2.3, the sulfamethoxazole degradation is measured at an absorbance of 260 nm. Maximal absorbance of sulfamethoxazole is observed at this wavelength as shown in Figure 11. The spectra of the samples at various pH are also shown. The samples are considered in steady-state as no more degradation is observed at the end of the reactions (this will be discussed more in depth in the next paragraph: 3.1.2) and the measurements have been done 1 week to 1 month after the reaction depending on the sample.

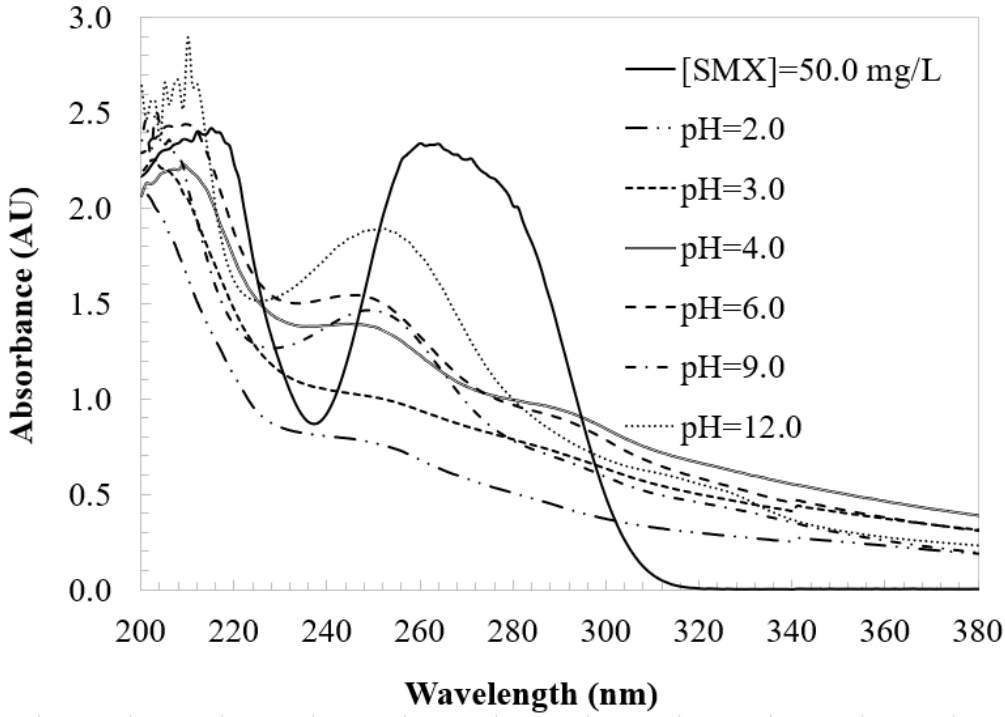

Figure 11: UV-spectra of sulfamethoxazole standard [50 mg/l] (full line) and steady state samples of the sulfamethoxazole degradation reactions at various pH

The peak around 260 nm lowers during the degradation of sulfamethoxazole, forming less aromatic compounds at first, which are then degraded as well. The pH has a significant effect in the result of the reaction. The signal at 260 nm is lower at steady-state for lower pH values, such as 2.0 and 3.0, while higher pH values have a higher residual signal. This can be attributed to either less degradation of sulfamethoxazole at higher pH or the formation of intermediates that interfere with the signal. A peak is visible around 254 nm, which can be explained by the formation of intermediates which are less aromatic (smaller resonance structure) than SMX and thus have a lower absorbance at 254 nm. It is interesting to note that the spectrum of the pH 12 sample shows an almost equal absorption at 254 nm than the sulfamethoxazole standard [50 mg/l]. Potentially this sample has a contamination (higher $[SMX]_0$ than 50 mg/l or contamination from unclean equipment) or the degradation of the less aromatic compounds occurred slower than their formation, causing accumulation of these aromatic compounds. The measurements of

sulfamethoxazole, turbidity, aromaticity and color shown in the next paragraphs give more insight in the kinetics of these reactions.

Figure 12 shows the SMX oxidation kinetics plotted as a function of the normalized concentration values ($[SMX]/[SMX]_0$), together with the loss of aromaticity of water ($[A_{254}]/[A_{254}]_0$) and dissolved oxygen ($[DO]/[DO]_0$). As can be seen, the SMX concentration decreases exponentially with time until it reaches a plateau, showing that, as SMX oxidizes, the aromaticity of the water decreases. This is due to the fact that SMX degrades to species with a smaller resonance structure. In terms of thermodynamic stability, open-chain compounds are treated as less stable than the SMX molecule, which contains a benzene ring in its molecular structure.

In turn, during the first 30 min of reaction, the initial concentration of dissolved oxygen decreases from [DO] 0 =8.0 mg L^{-1} to [DO]=5.4 mg L^{-1} . This is caused by the strong oxidizing conditions in the system, which cause a consumption of the dissolved oxygen in the water through oxidation reactions with organic matter. During this first stage, a high load of oxidizing radicals is generated in the system that degrade the pollutant load in the water. Literature shows that a decrease in the concentration of dissolved oxygen to near zero indicates a lack of hydrogen peroxide (Santos-Juanes et al., 2011). This would indicate that the concentration of hydrogen peroxide used in the treatment would have been used in the oxidation process (Villota et al., 2021). Next, a slower oxidation stage takes place, because much of the hydroxyl radicals have been consumed, and radical species of lower oxidizing power are generated, which slowly decreases the oxidizing power and thus slowly degrades the organic matter. During this stage the DO concentration remains practically constant.

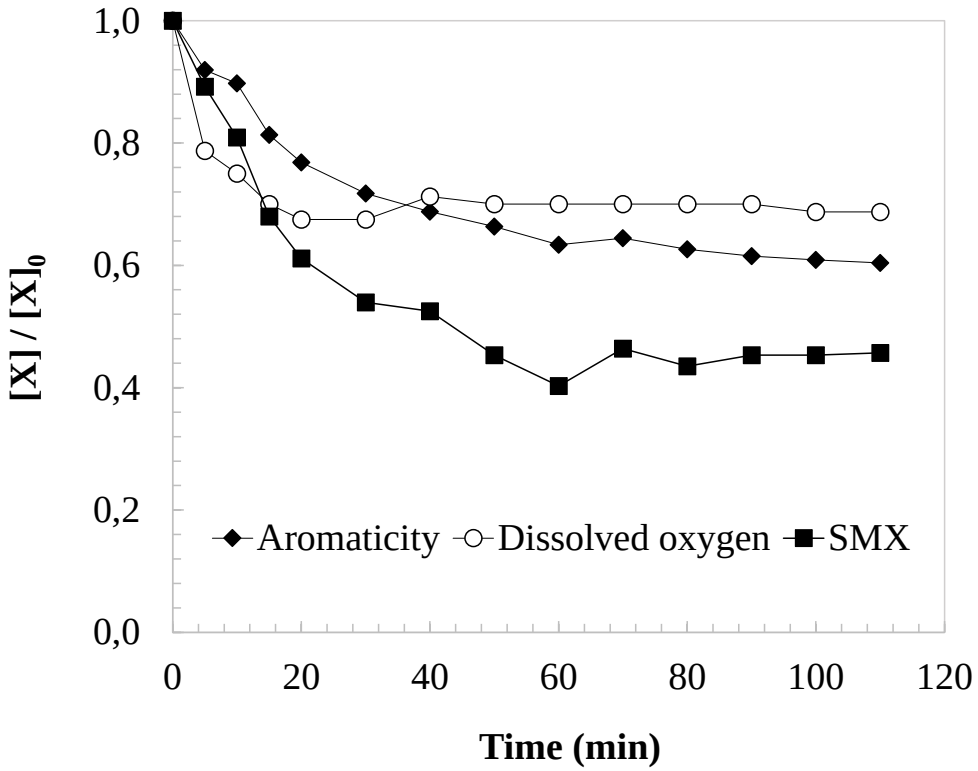

Figure 12: Normalized kinetics of sulfamethoxazole [SMX] (mg L $^{-1}$), aromaticity. Experimental conditions: [SMX]$_0$=50.0 mg L-1; [H_2O_2]$_0$=100.0 mM; [UV]=150 W; T=25ºC; [A_{254}]$_0$=2.34 AU; [DO]0=8.0 mg L^{-1}

On the other hand, during the oxidation of aqueous SMX solutions, a strong brown color is generated in the water, which is accompanied by high turbidity formation (up to 40 NTU). Figure 13 shows the kinetics of color and turbidity formation during SMX degradation using oxidant molar ratios of the order of 500 mol H_2O_2/mol SMX and operating at pH=4.0, which are the conditions that lead to the highest levels of color and turbidity in the treated water. It is observed that both color and turbidity increase rapidly during the first 30 min of the reaction, until reaching a plateau.. This evolution would indicate that the colored intermediates that contribute to the turbidity of the water are generated during the first minutes of the oxidation of SMX, as a consequence of the strong radical attack of the hydroxyl radicals.

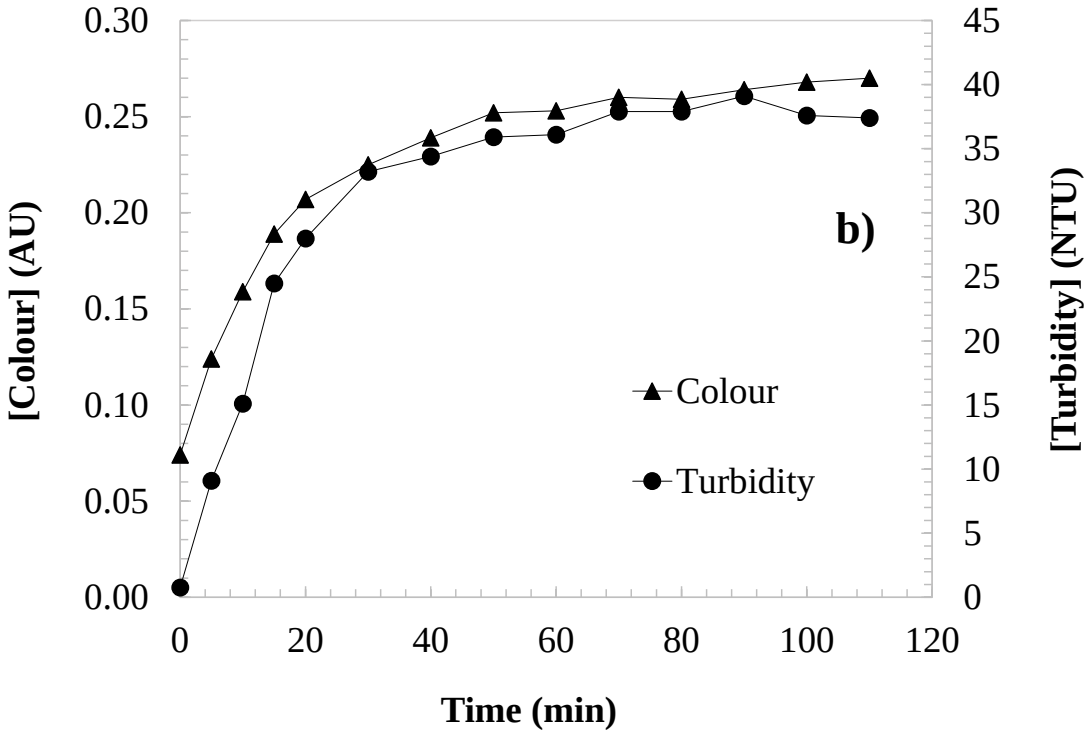

Figure 13: Kinetics of color [Color] (AU) and turbidity [Turbidity] (NTU) during the SMX oxidation by UV/H_2O_2 conducting at pH=4.0. Experimental conditions: $[SMX]_0$=50.0 mg L^{-1}; $[H_2O_2]_0$=100.0 mM; [UV]=150W; T=25ºC; $[A_{254}]_0$=2.34 AU; [DO]0=8.0 mg L^{-1}

Studies reported in the bibliography on the oxidation of SMX using different AOPs, such as, adsorption processes (Kurup, 2012), nanofiltration membranes (Nghiem et al., 2008), carbon materials (Gonçalves et al., 2012), photocatalytics (Naraginti et al., 2018) or UV technology (Lester et al., 2010) do not refer to these phenomena. Therefore, this study will model and explain the causes of color formation and the causes of color and turbidity formation in water based on the SMX degradation mechanism.

The control of turbidity is of special importance, because it is directly related to the effectiveness of disinfection processes, whether chemical (chlorine or other biocides) or physical (UV radiation). Directive (EU) 2020/2184 on the quality of water intended for human consumption indicates that turbidity is a parameter that must be controlled in water supply installations and must not exceed 1 NTU. According to Regulation (EU) 2020/741 on minimum requirements for water reuse, among the quality requirements for reclaimed water for agricultural irrigation, the water obtained from secondary treatment, filtration and disinfection must have turbidity levels ≤ 5 NTU.

3.1.2. Kinetic modelling of SMX degradation

Figure 14 shows the normalized measured absorbance at 260 nm during the reactions at different pH with a fitted pseudo first-order model.

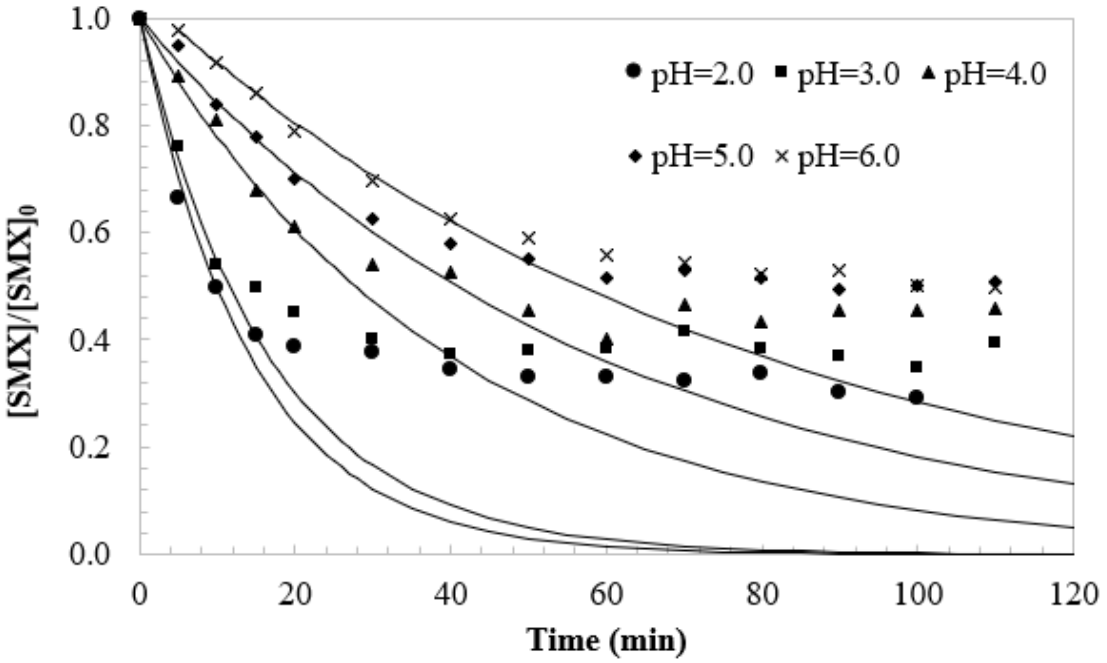

Figure 14: Measured absorbance at 260 nm at various pH and proposed second order kinetic model of SMX degradation

It is important to note that the reaction is not complete, as a plateau is formed at a maximum of 60% conversion (pH 2.0 reaction). The H_2O_2 concentration has depleted enough for the reaction to stop. For this reason the first 20 seconds of the reactions are observed to determine the reaction order. Figure 15 shows the reaction rate in function of time for the reaction at pH 2.0.

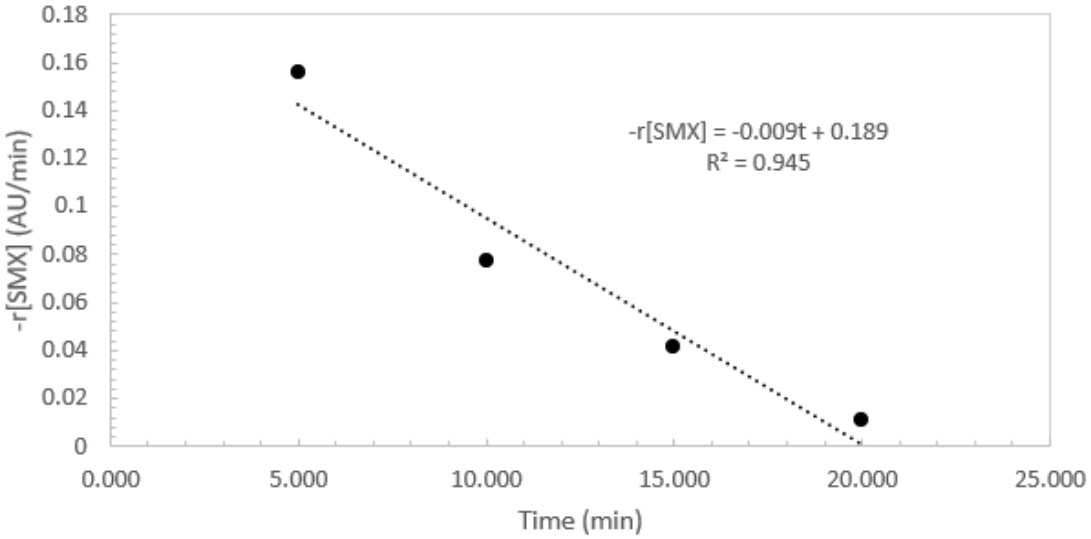

Figure 15: Reaction rate for the first 20 seconds of the reaction at pH 2.0

A linear correlation indicates a first order reaction, however in this case there is a small change in reaction rate as the concentration of the reactants change, which would indicate a second-order reaction. On the other side, it is also possible to assume first-order reaction kinetics, as Figure 16 exemplifies:

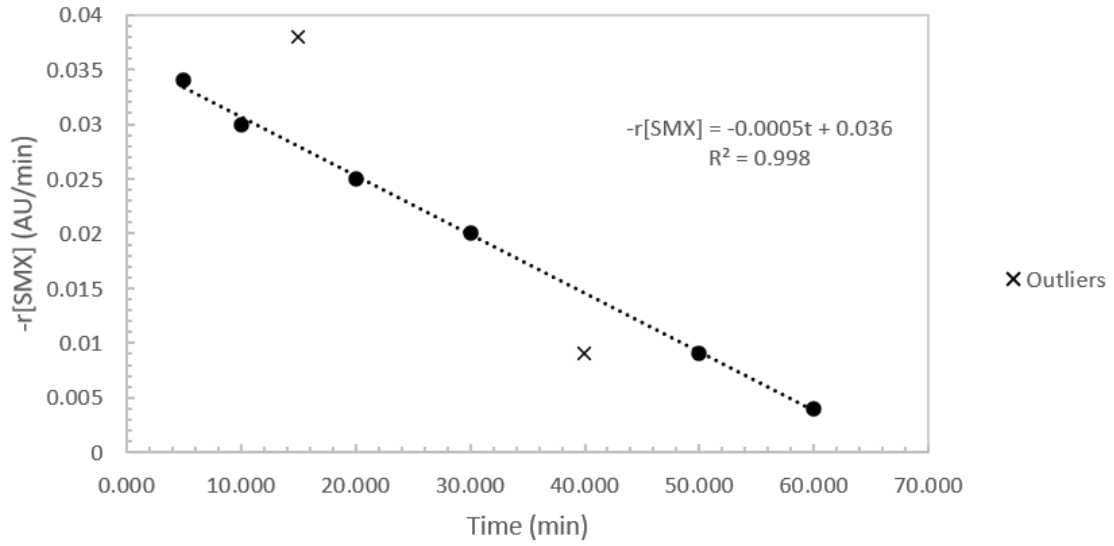

Figure 16: Reaction rate for the first 60 seconds of the reaction at pH 6.0

Examination of the reaction rate of the other reactions provides similar inconclusive results. In literature, it can be found that hydroxyl radicals and sulfonamide antibiotics react together with second order kinetics (Borowska et al., 2015; R. Zhang et al., 2016). Other research has modelled the UV/H_2O_2 reaction of sulfamethoxazole as pseudo first-order, assuming a constant effect of the hydroxyl radical concentration (Hollman et al., 2020; Martínez-Costa et al., 2018; Zhu et al., 2019). For the UV/H_2O_2, an excess of H_2O_2 was used (100 mM). Thus, a pseudo first-order kinetic model is proposed for the degradation of sulfamethoxazole in water (Eqs. 1-2), where the reverse reaction is negligible and the kinetic constant is expressed as a function of the applied pH (Eqs. 3-4):

$$-\frac{d[SMX]}{dt} = k_{real}\,[SMX] * [OH°] = \; k_{SMX}\,[SMX] \tag{1}$$

$$[SMX] = [SMX]_0 * \exp\,(-k_{SMX} * t) \tag{2}$$

with,
$[SMX]_0$: Initial measurement of SMX in aqueous solutions(AU)
$[SMX]_\infty$: SMX in the oxidized samples in the steady state (AU)
k_{SMX}: pseudo-first-order rate constant for degradation of SMX in water (min $^{-1}$)

$$[SMX]_0 = (2.64 \pm 0.19)\; AU \tag{3}$$

$$k_{SMX} \; = 0.003\;(pH)^2 - 0.038pH + 0.139;\; (r^2{=}0.940) \tag{4}$$

Figure 17 and Figure 18 show the kinetic constants in function of pH:

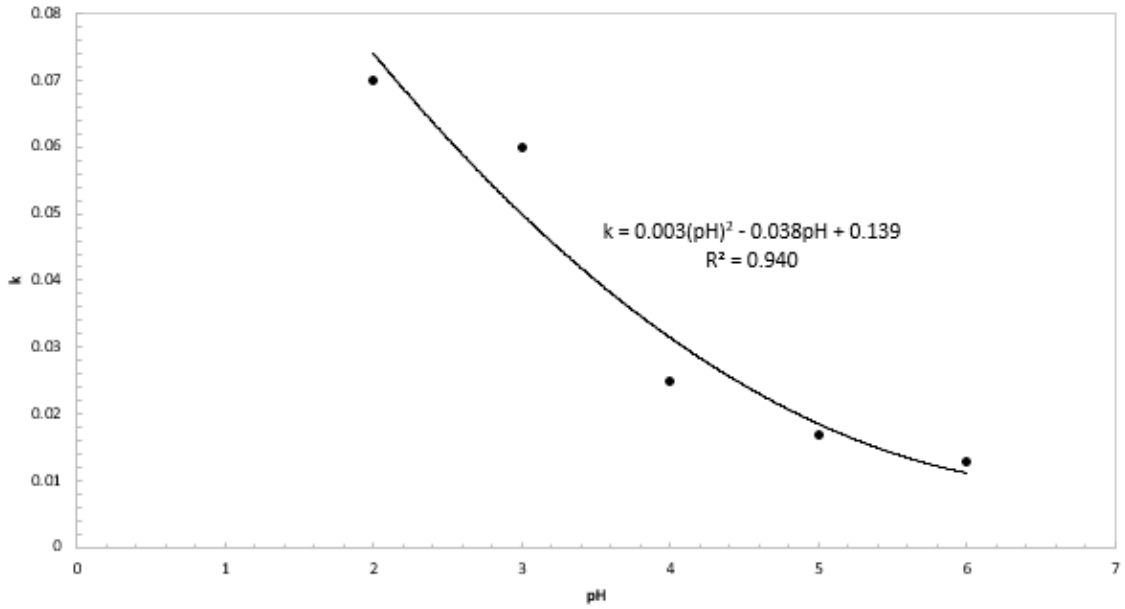

Figure 17: Kinetic constants of second order SMX model in function of pH

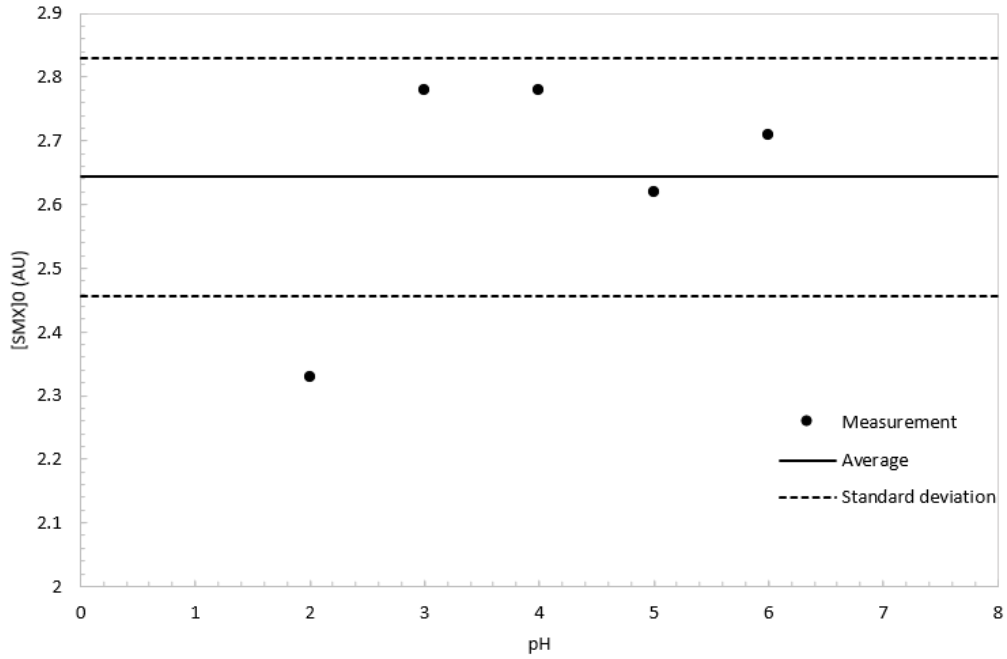

Figure 18: Initial SMX measurements in function of pH

The degradation occurs slower at higher pH, this is reflected in the downward trend of the kinetic constant (Figure 17). The rate at which hydroxyl radicals react with the pollutants does not change, as it is diffusion limited. This means that a slower formation of hydroxyl radicals occurs at a higher pH. One possible explanation is a slower propagation in the reactions that form OH^-. Due to the higher concentration of hydroxyl ions at higher pHs, the equilibrium is shifted and a slower reaction occurs.

The initial sulfamethoxazole (Figure 18) measurement remains constant around an average value. This is logical as no reaction has occurred yet. The initial absorbance,

shown in Figure 18, averages around 2,64 with a standard deviation of 0,19. This variance is on the one hand caused by the sum of human errors during the creation of the solution and the inherent variance of the spectrophotometer. On the other hand this variance is caused by the slow degradation of SMX during storage of the initial SMX solution. These SMX solutions were stored for a maximum of 3 days at room temperature, but this can result in a 22% loss of sulfamethoxazole in the solution (Shoaib Khan & Sajid Ur Rehman, 2012). Also important to note is the effect of H_2O_2 on the measurement. Measuring the absorbance without a separation step such as HPLC makes for an aselective measurement. Any compound which absorbs wavelength at 260 nm will affect the measurement. The UV/VIS spectrum of 8.8M H_2O_2 is shown in Figure 19:

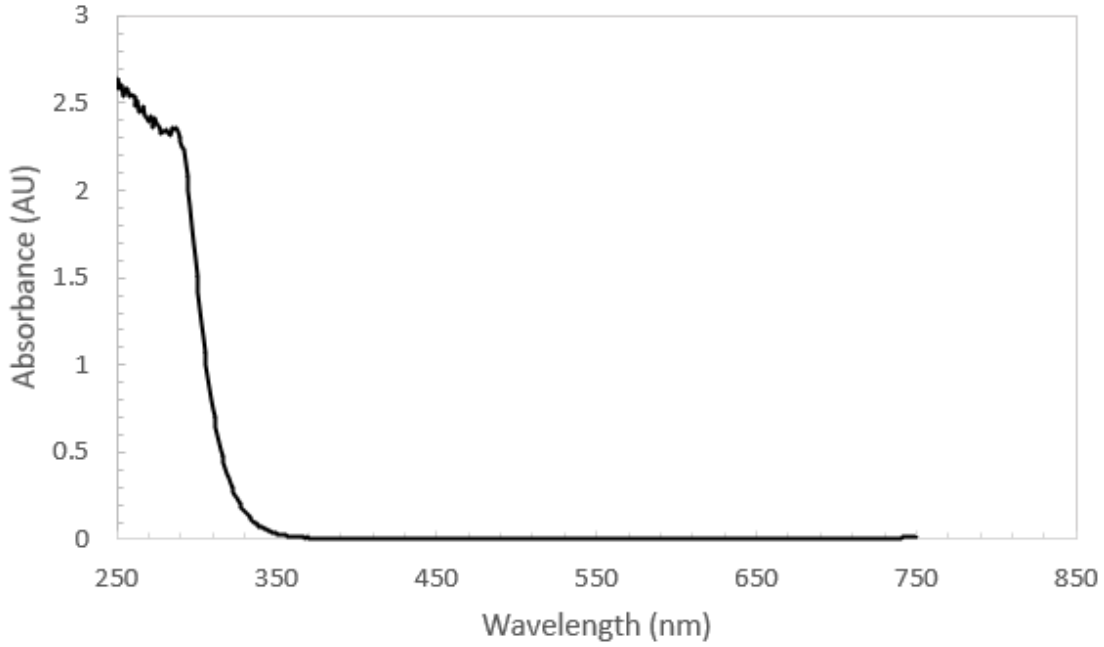

Figure 19: UV/Vis absorption spectrum of 8.8M H_2O_2

The signal clearly interferes with the measurements at 254 nm and 260 nm. The low initial value of the SMX measurement can be explained with this in mind. If the sample at t=0 is taken before addition of H_2O_2 to the reactor, then a lower absorption value will be measured than when a sample is taken after the addition of H_2O_2. During the tests it was not realized that H_2O_2 could have this effect. Nevertheless, a pseudo first-order model fits the degradation measurements well, which leads to believe that the effect of H_2O_2 is not extreme enough to discard the results.

3.1.3. pH effect on SMX oxidation by UV/H_2O_2

Table 3 shows the results of the ionic chromatography on the steady state samples ($[SMX]_0$=50 mg/l). Relevant results are graphically illustrated together with steady state results of color, turbidity and SMX degradation in Figure 20, Figure 21, Figure 24 and Figure 25:

Table 3: Ionic chromatography results of steady-state samples of UV/H_2O_2 reactions at various pH. ND = Not detected; ACL = Above calibration line; BDL = Below detection limit

pH	Quinones ppm	Acetic acid ppm	Pyruvic acid ppm	Chloric acid ppm	Nitric acid ppm	Succinic acid ppm	Malic acid ppm	Malonic acid ppm	Maleic acid ppm	Sulfuric acid ppm	Oxalic acid ppm
2	ND	6.526	ND	ACL	ND	ND	ND	ND	ND	10.386	1.532
3	ND	2.861	ND	18.891	0.490	ND	ND	ND	ND	10.196	BDL
4	ND	3.039	ND	34.378	ND	ND	ND	ND	ND	9.349	BDL
5	ND	4.042	ND	8.882	2.668	ND	ND	ND	ND	6.814	ND
6	ND	3.183	ND	41.153	3.699	ND	ND	ND	ND	5.734	ND
9	ND	5.713	ND	9.437	ND	ND	ND	ND	ND	4.829	ND
12	ND	8.604	ND	ACL	3.505	ND	ND	ND	ND	4.998	1.884

The pH is a significant parameter in advanced oxidation processes as it determines the production of oxidizing radicals (Boutiti et al., 2017). It is found that the efficiency of the UV/H_2O_2 oxidation process lies in the stoichiometric formation of two hydroxyl radicals from the photocatalytic decomposition of H_2O_2 (García, 2007). In this work, the effect of carrying out SMX oxidation at controlled pH on the process efficiency and SMX degradative pathways has been studied, operating within a pH range between 2.0 and 12.0.

Figure 20 shows the SMX oxidation and aromaticity loss (%) of the treated waters as a function of pH once the steady state is reached. The results show that the more acidic the pH at which the treatment is carried out, the lower the SMX concentration and aromaticity of the treated water. As the operating pH becomes more basic, the conversions obtained are lower than at acid pH. Thus, operating at pH=2.0, the highest SMX degradation (74%) and aromaticity loss (64%) rates are obtained. Operating at pH=12.0 decreases the efficiency of the treatment, obtaining 40% for loss of aromaticity and 35% for SMX oxidation. Similar results have been obtained in studies reported in the literature, where a higher reaction rate was observed in acid solution (Liu et al., 2019).

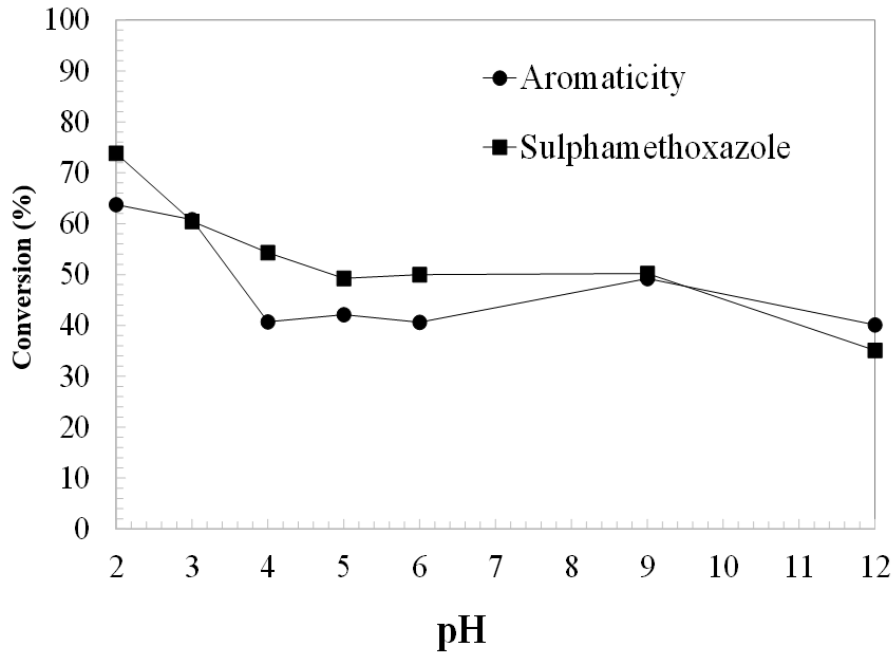

Figure 20: Aromaticity and sulfamethoxazole at steady-state in function of pH

Figure 21 shows the color and turbidity of the oxidized water at the different pH values tested. The color increases from pH=2.0, where the oxidized water shows a light yellow appearance, until it reaches a maximum value at pH=4.0, characterized by a dark brown color. At a pH higher than 4.0, the color decreases with pH, obtaining a light yellow color again at pH=12.0. This color change over the pH range at steady-state is also shown in Figure 22.

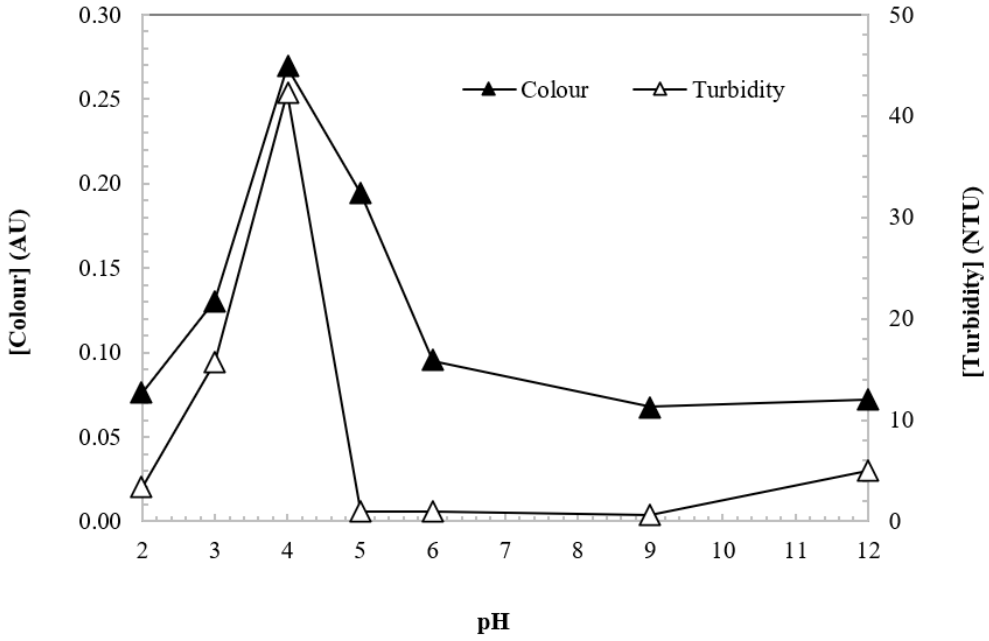

Figure 21: Color and turbidity measurements at steady state in function of pH

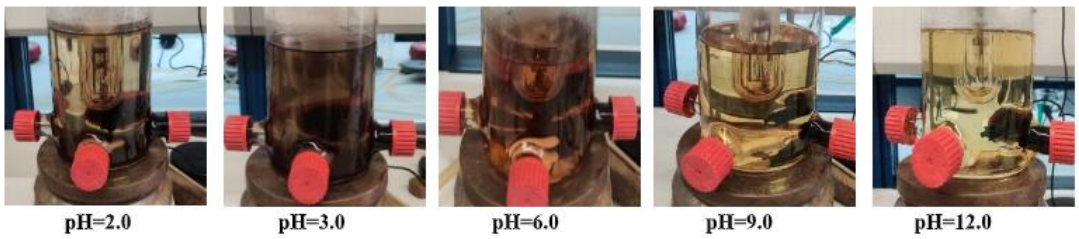

Figure 22: Color of SMX oxidized aqueous solutions as a function of pH value. Experimental conditions: [C]0=50.0 mg L-1; [H_2O_2]0=100.0 mM; [UV]=150 W; T=25°C.

To explain this phenomenon, it is necessary to consider the conjugated acid and base of SMX as a function of pH (Carrizales, 2020; Qiang & Adams, 2004; Wu et al., 2010) because the pH of the solution can affect the chemical form of dissociable compounds. SMX exists in positive, neutral and negative forms, as it has two amino groups that can be ionized. In Figure 23 it can be seen that SMX at pH<3.0 is mostly in its cationic form due to protonation of the amino group, while at pH between 4.0 and 6.5 it is mostly in its neutral and partially anionic form, and at pH>8.0 its anionic form dominates due to deprotonation of the amide nitrogen, where almost all SMX molecules in water are dissociated and negatively charged.

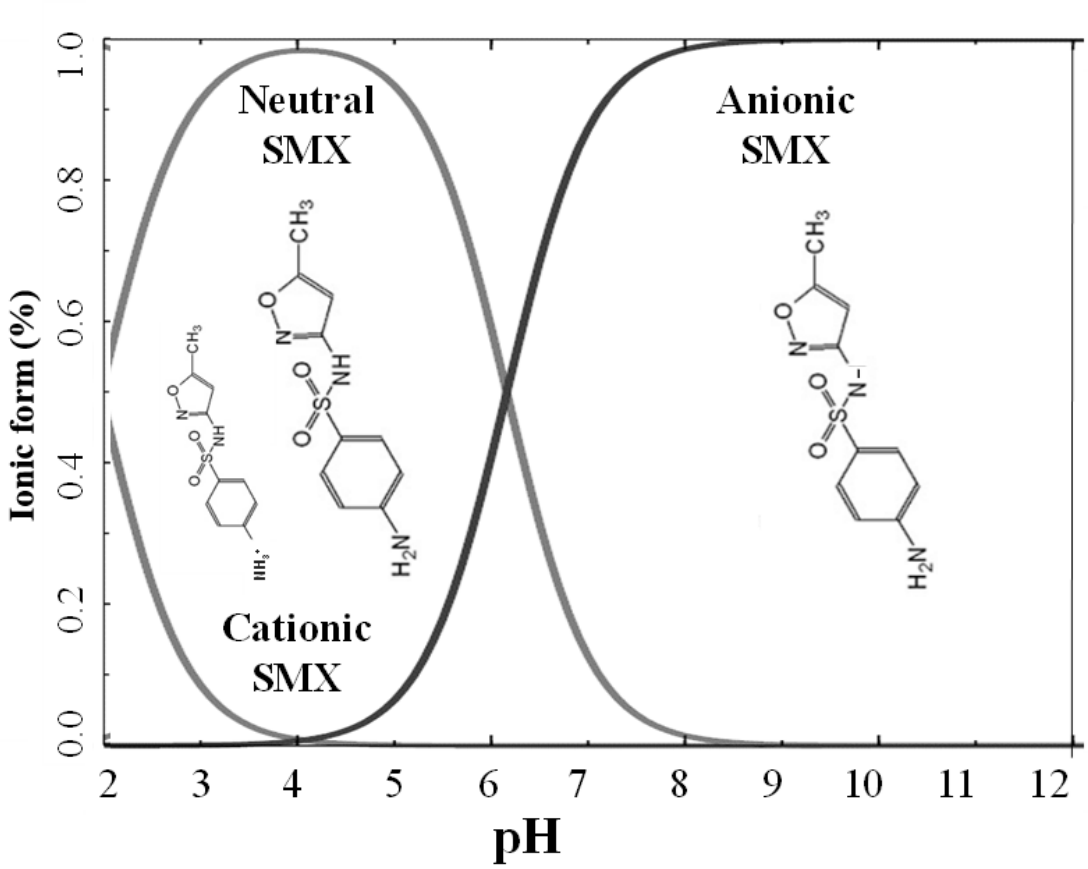

Figure 23: SMX ionization percentage in function of pH

Within the operating range between pH=2.0 and 4.0, it is observed that as the cationic form of SMX decreases with respect to the neutral SMX molecule, brown color is formed in the water, reaching the maximum color value at pH=4.0, when 100% of the SMX is in its neutral form. This would indicate that the oxidation of SMX in its neutral form would take place through degradation to strongly colored intermediates. Operating in the interval between pH=4.0 and 12.0, it is found that as the neutral form of SMX decreases and the proportion of anionic SMX increases, the color decreases, until pH values above 8.0, when the percentage of neutral SMX is 0%. Light yellow waters are observed at pH values above 8.0. Analyzing turbidity, it is observed that significant levels of turbidity are generated when operating at pH=3.0 (16 NTU) and 4.0 (42 NTU). These values indicate that the turbidity-causing species are generated from the degradation of SMX in its neutral state. Turbidity is also generated, although to a lesser extent, if neutral SMX is in equilibrium with cationic SMX. However, the anionic SMX molecule does not generate turbidity in water, even if it is in equilibrium with neutral SMX.

To analyze the SMX degradation pathways causing color and turbidity in water, studies reported in the literature on the oxidation of aqueous pollutants with UV/H_2O_2 technology have been considered, which show a drastic variation of intermediates with the solution pH (Liu et al., 2019). Based on these, some of the degradation intermediates detected in the oxidized samples were analyzed (see Figure 24 and Figure 25). In view of the results,

the formation of carboxylic acids (acetic acid and oxalic acid) and two inorganic species (sulfate ions and nitrate ions) have been detected.

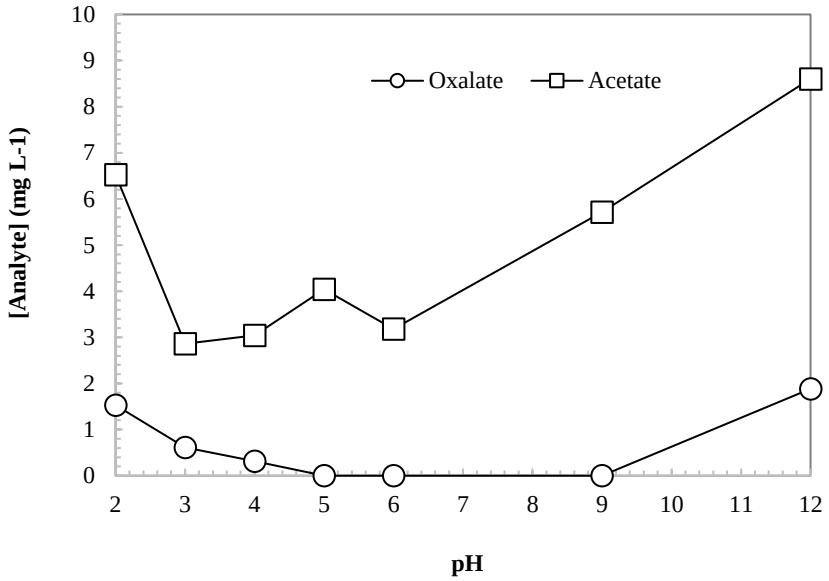

Figure 24: Oxalate and acetate at steady state in function of pH

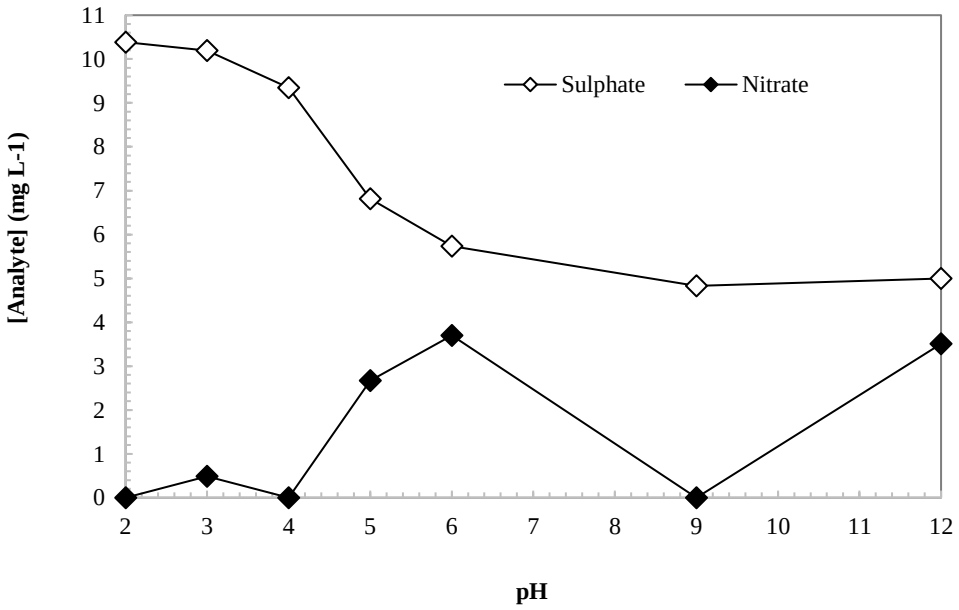

Figure 25: Sulphate and nitrate at steady state in function of pH

Figure 24 shows that the oxidation of SMX to the formation of oxalic acid and acetic acid is favored at pH=2.0 and pH=12.0, where light yellow water is obtained. Under these operating conditions, the opening of the aromatic rings takes place. Operating at pH values between 3.0 and 6.0, when the formation of brown color in the water takes place, the formation of carboxylic acids is minor, which would indicate that, when color is produced in the water, the oxidation treatment would not reach SMX degradation levels that lead to the opening of the aromatic rings.

As can be seen in Figure 25, concentration of sulfate ions analyzed in the treated water decreases as the pH of the medium becomes more basic. This may be due to the fact that, operating at acidic pH, the concentration of H^+ protons in the medium is higher. The protons would be added to a carbon of the benzene ring, leading to desulfonation reactions, in which SO_3 and benzene would be formed. The sulfur trioxide generated would react with water, leading to the formation of sulfate ions as shown in Figure 26:

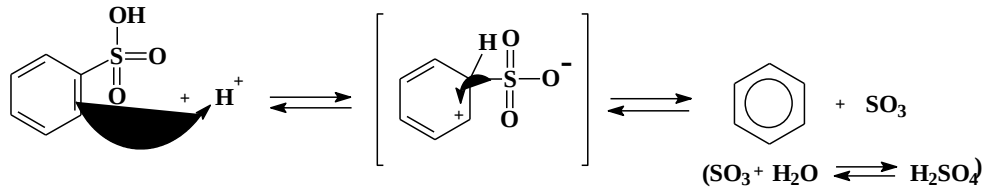

Figure 26: Proposed desulfonation of sulfamethoxazole in acid conditions

The concentration of nitrate ions analyzed in the water samples shows its maximum formation at pH=6.0, when the proportion of neutral SMX in relation to anionic SMX is 50%. However, at pH=4.0 the presence of nitrate ions in the water is not detected. This fact would indicate that when the formation of color and turbidity in the water is at its maximum, the mineralization of SMX degradation intermediates that have substituted nitrogen atoms in their molecular structure does not take place.

3.1.4. Kinetic modelling of aromaticity

Figure 27 shows the measured absorbance at 254 nm during the reactions at different pH:

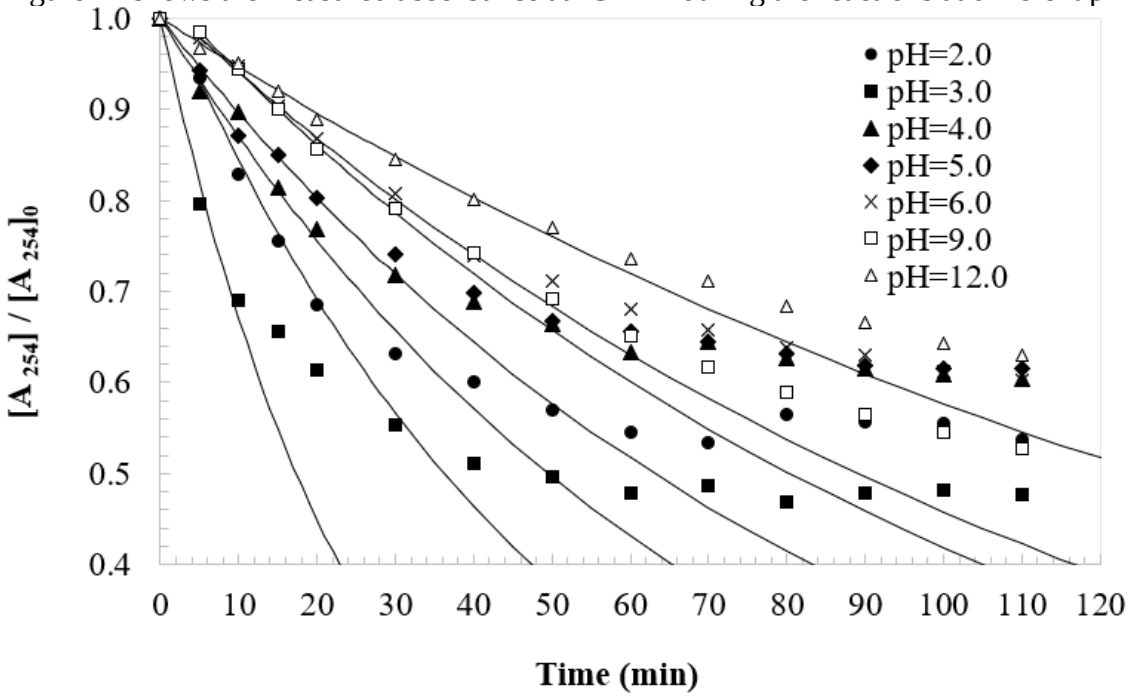

Figure 27: Measured aromaticity at various pH and proposed pseudo first-order kinetic model of aromaticity degradation

Again, a plateau is formed before the model reaches the end of the reaction. At around 70% to 75% the effect of the lowered concentration of hydroxyl radicals starts playing a role and the reaction slows down. The pseudo first-order model ignores this effect. To create a complete model the hydroxyl radical concentration should be known, for which no tools were available.

Figure 28 shows the reaction rate of the aromaticity degradation of the reaction at pH 5.0 to illustrate that, similar to the SMX degradation, the aromaticity degradation can also be modelled by both pseudo first-order and second order kinetics.

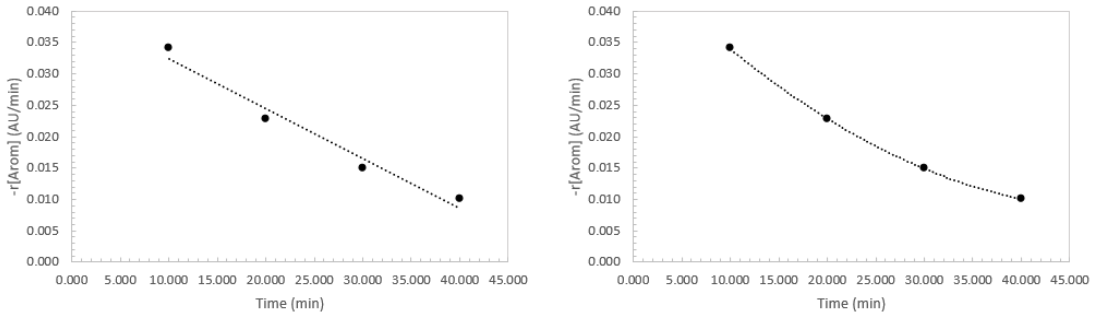

Figure 28: Reaction rate of aromaticity degradation of the reaction at pH 5.0 with linear fit (left) and 2nd order polynomial fit (right)

Since the aromaticity degradation is linked to the degradation of SMX, a pseudo first-order kinetic model is proposed for the removal of aromaticity from the water (Eqs. 5-6), where the kinetic parameters are expressed as a function of the applied pH (Eqs. 7-8):

$$-\frac{d[A_{254}]}{dt} = k_{real}\,[A_{254}] * [OH°] = \; k_{A_{254}}\,[A_{254}] \tag{5}$$

$$[SMX] = [SMX]_0 * \exp\,(-k_{SMX} * t) \tag{6}$$

with,
$[A_{254}]_0$: Initial measurement of color in aqueous solutions (AU)
$[A_{254}]_\infty$: Color in the oxidized samples in the steady state (AU)
$k_{A_{254}}$: pseudo-first-order rate constant for formation of color in water (min $^{-1}$)

$$[A_{254}]_0 = (2.487 \pm 0.410)\; AU \tag{7}$$

$k_{A_{254}}$ => No linear or second order trend for the kinetic constant in function of pH (8)

Figure 29 and Figure 30 show the kinetic parameters in function of pH:

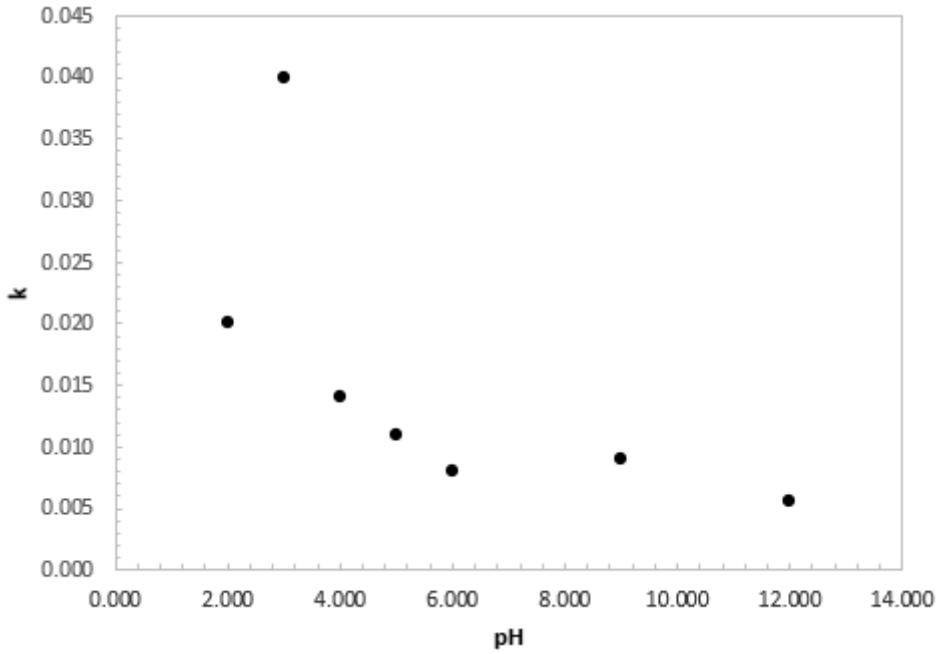

Figure 29: Kinetic constants of pseudo first-order aromaticity model at various pH

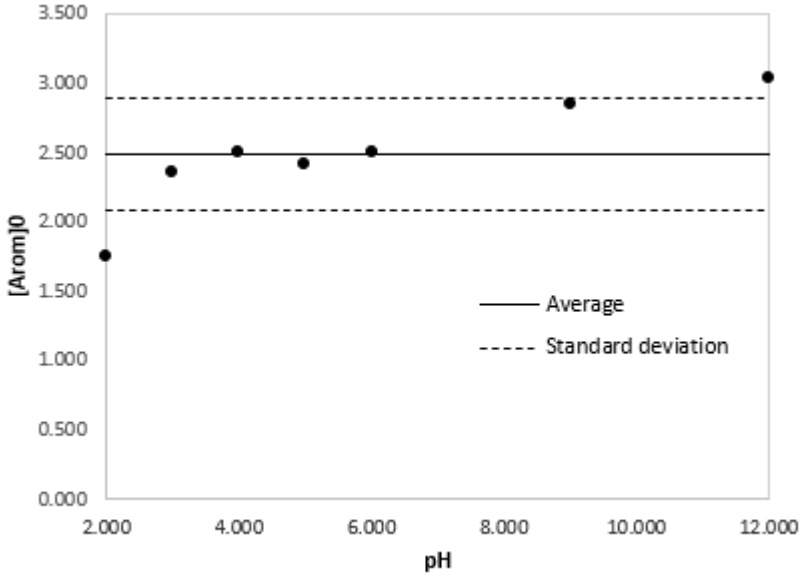

Figure 30: Initial aromaticity measurement in function of pH

Figure 29 shows that the removal of aromaticity is more effective at lower pH values, with a maximum at pH 3 and a steep drop in speed of aromaticity removal after. This can be linked to the degradation of SMX during the reaction, which also slows down at higher pH values. It is interesting to note that, while the SMX degradation is fastest at pH 2.0, the aromaticity degradation slows down at a pH of 2.0. This could be linked to the desulfonation reaction for low pH values shown in Figure 26. It could also be caused by a mistake during the measurements of the pH 3.0. reactions, which caused a change in aromaticity measurement, but not in SMX measurement as a significant increase in degradation speed is not expected at pH 3.0 (Yang et al., 2017).

3.1.5. Kinetic modelling of color formation

Figure 31 shows the color measurements during the entire reaction at various pH:

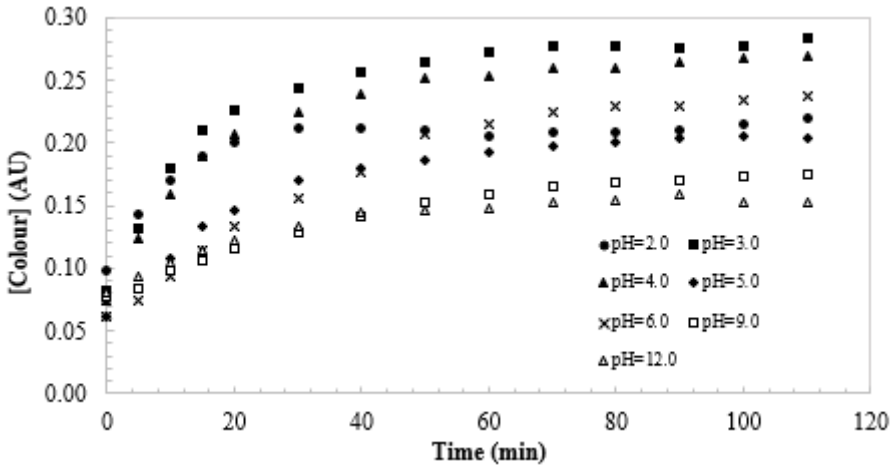

Figure 31: Color formation in function of time for reactions at various pH

The color is caused by the formation of a reaction intermediate. The formation of this intermediate is dependent on, in this case, the pseudo first-order degradation of sulfamethoxazole by hydroxyl radicals (Eqs. 9-11).

$$\frac{d[A_{455}]}{dt} = \frac{-d[SMX]}{dt} = k_{real}\,[SMX] * [OH°] = \; k_{SMX}\,[SMX] \tag{9}$$

$$[A_{455}] = [A_{455}]_0 + k_{SMX} * [SMX] * dt \tag{10}$$

$$[A_{455}] = [A_{455}]_0 + k_{Obs} * \frac{[SMX]}{[SMX]_0} * dt \text{ with } k_{Obs} = k_{SMX} * [SMX]_0 \tag{11}$$

Figure 32 shows the color measurements with the fitted pseudo first-order model. The model was not made for pH 9.0 and 12.0 since absorbance at 260 nm ([SMX]) was not measured for these reactions. Figure 33 and Figure 34 show the kinetic constants in function of the pH:

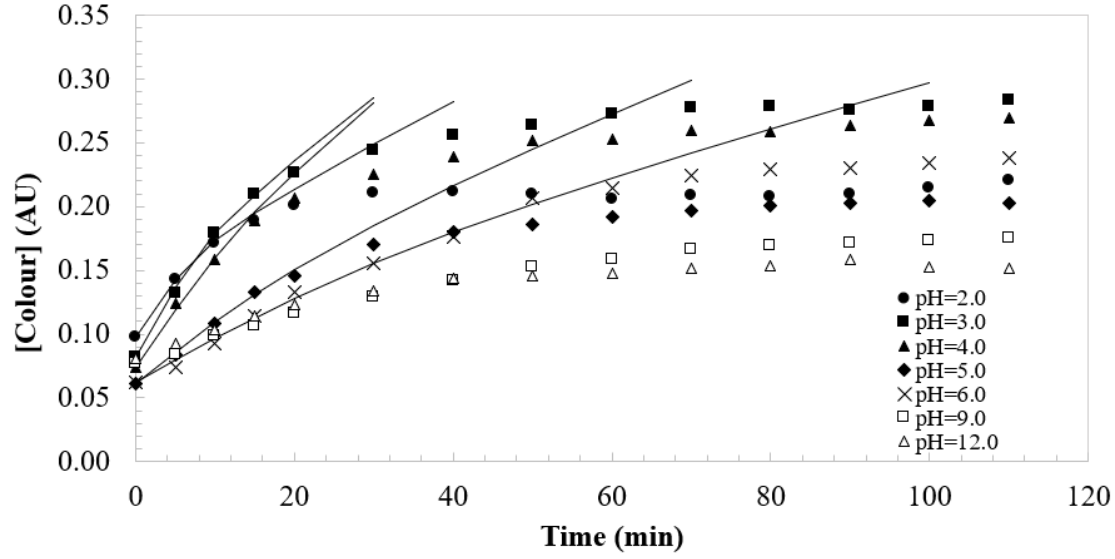

Figure 32: Color formation in function of time for reactions at various pH with fitted pseudo first-order model

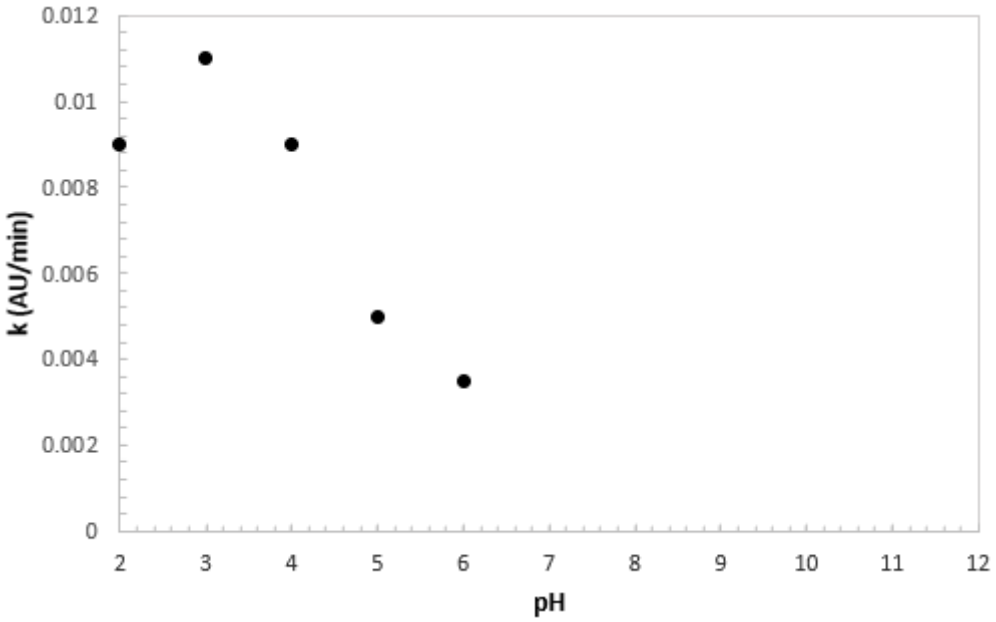

Figure 33: Kinetic constant of color formation at varying pH

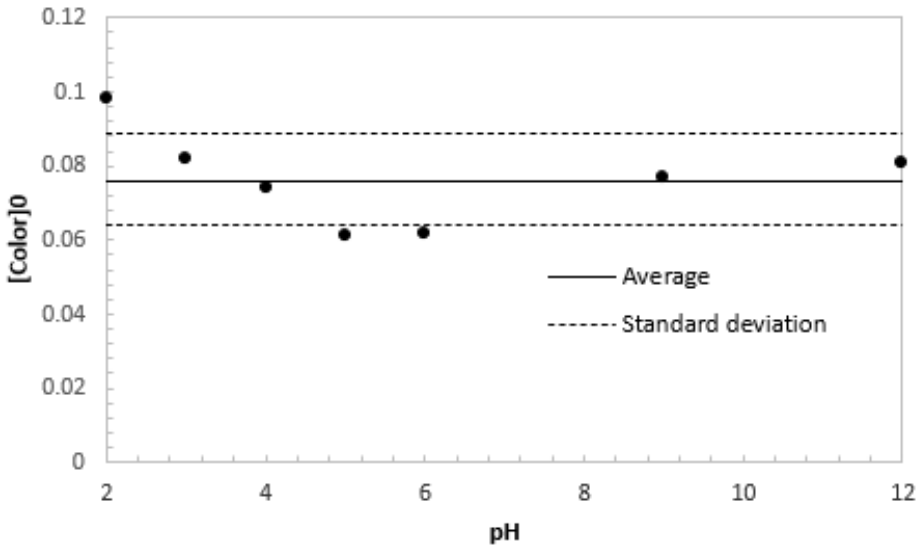

Figure 34: Initial color measurements for the reactions at varying pH

The kinetic constant, shown in Figure 33, peaks at pH 3.0 and decreases when the pH decreases or increases. The color formation depends on the formation of color absorbing intermediates. The observed phenomena can be explained by a slower formation of these intermediates when sulfamethoxazole is positively or negatively charged. The intermediate itself could also become charged and then produce less or no color, depending on the compound formed.

3.1.6. Kinetic modelling of turbidity formation

The turbidity is caused by the formation of a reaction intermediate. The formation of this intermediate is dependent on, in this case, the pseudo first-order degradation of sulfamethoxazole by hydroxyl radicals (Eqs. 12-14).

$$\frac{d[NTU]}{dt} = k_{real}\,[SMX] * [OH°] = \; k_{SMX}\,[SMX] \tag{12}$$

$$[NTU] = [NTU]_0 + k_{SMX} * [SMX] * dt \tag{13}$$

$$[NTU] = [NTU]_0 + k_{Obs} * \frac{[SMX]}{[SMX]_0} * dt \text{ with } k_{Obs} = k_{SMX} * [SMX]_0 \tag{14}$$

Figure 35 shows the turbidity during the reaction with a pseudo first-order model. No model was created for the reactions at pH 9.0 and 12.0, as no measurements were made at 260nm for these samples. Figure 36 and Figure 37 show the kinetic constants in function of pH:

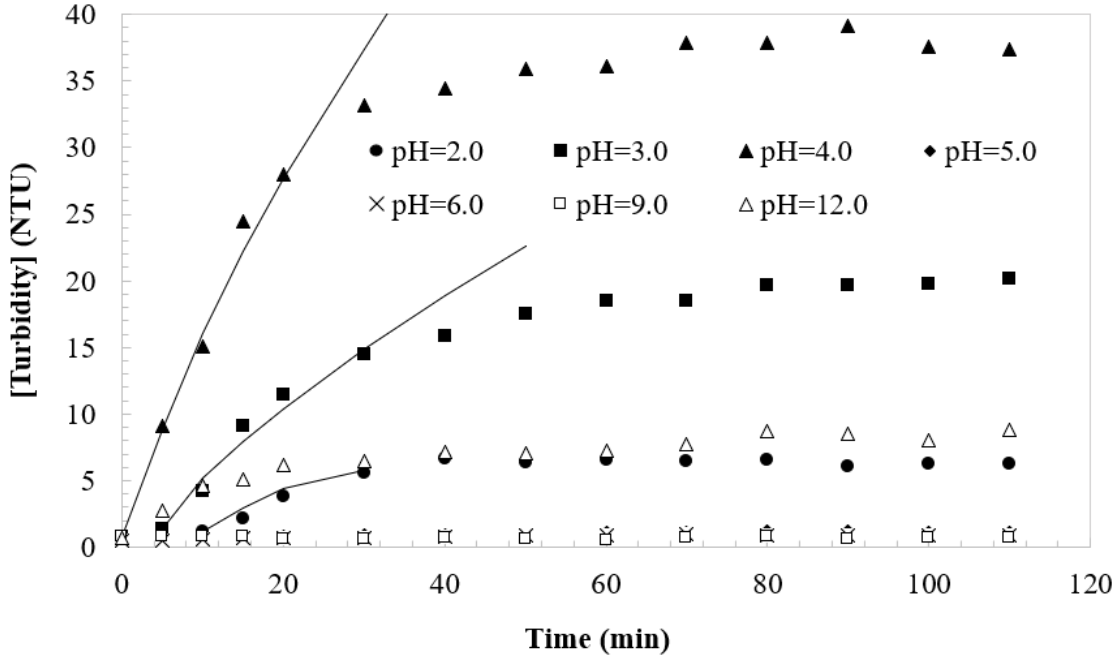

Figure 35: Turbidity formation during the reaction with fitted pseudo first-order model

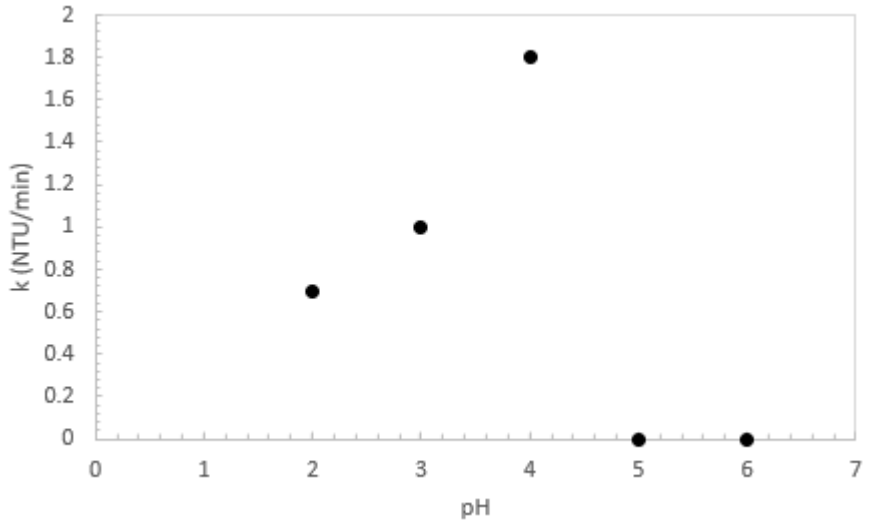

Figure 36: Pseudo first-order kinetic constant of turbidity formation in function of pH

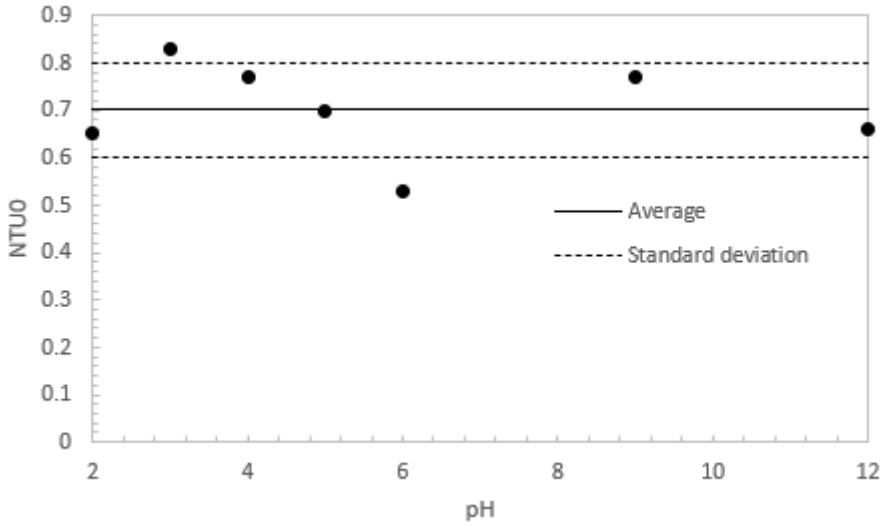

Figure 37: Initial turbidity measurements of the reactions at varying pH

The turbidity formation changes drastically depending on the pH. In paragraph 3.1.3 this was attributed to the ionization of SMX and the resulting variation in degradation pathway. The calculated kinetic constants reflect this, as the kinetic constant increases until pH 4.0, after which it drops to 0 since there is no reaction. The kinetic models are only valid for the first part of the reaction, because the reaction slows down too much without completing the full degradation of sulfamethoxazole, possibly due to slow formation of hydroxyl radicals or interference in the signal at 260 nm caused by other compounds.

3.2. PHOTO-FENTON REACTIONS

3.2.1. Sulfamethoxazole degradation

Figure 38 shows the reaction rate of the reaction with 10 mM H_2O_2 and 1 ppm Fe2+ in function of time. A non-linear trend is clearly visible and thus it is assumed that the photo-Fenton degradation of SMX follows second-order kinetics until the reaction stops.

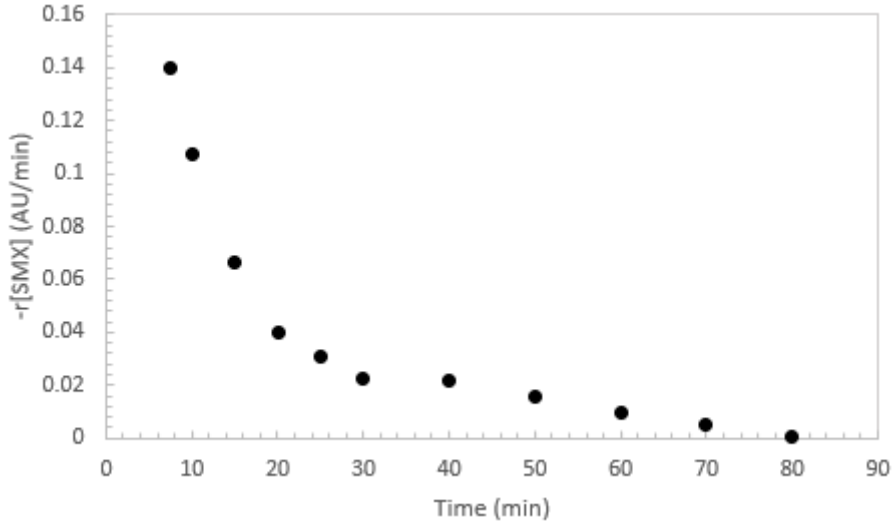

Figure 38: Reaction rate of SMX degradation for the reaction with [H_2O_2]=10 mM and [Fe^{2+}]=1 ppm

$$-\frac{d[SMX]}{dt} = k_{SMX}\,([SMX]^2) \tag{15}$$

$$\frac{1}{[SMX]} - \frac{1}{[SMX]0} = -k_{SMX} * t \tag{16}$$

$$[SMX] = \frac{1}{-k_{SMX}*t+\frac{1}{[SMX]0}} \tag{17}$$

3.2.2. SMX degradation: effect of Fe^{2+}

Figure 39 shows the SMX degradation at varying Fe^{2+} concentration, with a fitted second-order model. Figure 40 and Figure 41 show the kinetic constants and steady-state measurements in function of Fe^{2+} concentration.

$$[SMX]_0 = (2.585 \pm 0.055)\ AU \tag{18}$$

$$k_{SMX} = 0.015\,[Fe^{2+}] + 0.019;\ (r^2=0.976) \tag{19}$$

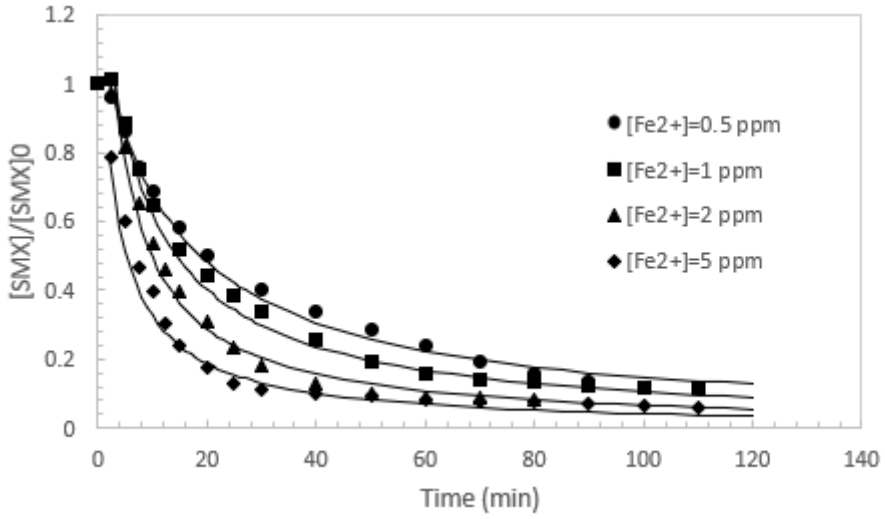

Figure 39: SMX degradation during the reaction for reactions with varying [Fe^{2+}]

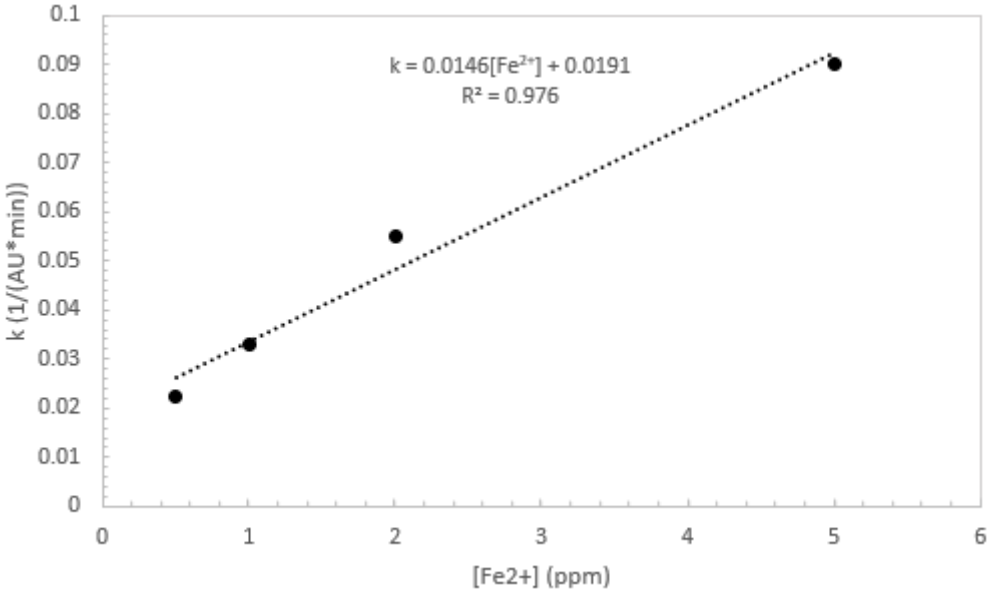

Figure 40: Second-order kinetic constant in function of [Fe^{2+}]

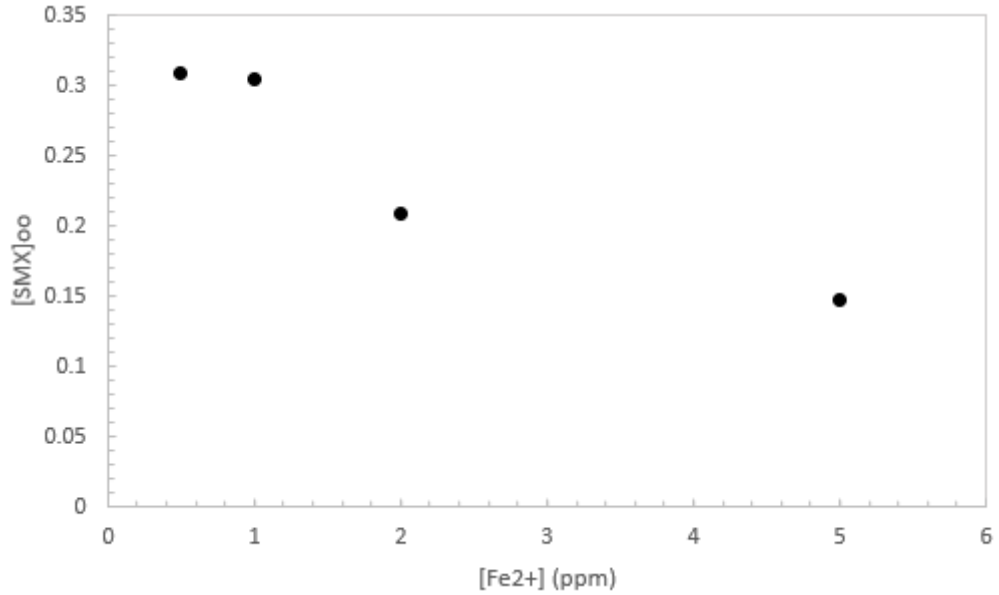

Figure 41: Steady-state SMX value in function of [Fe^{2+}]

The kinetic constant of the degradation of sulfamethoxazole increases linearly with the amount of Fe^{2+} in the solution. This linear effect begins to plateau at higher values of catalyst as seen on Figure 40.

3.2.3. SMX degradation: effect of H_2O_2

Figure 42 shows the SMX degradation at varying H_2O_2 concentration, with a fitted second-order model in Figure 43. The model is the same as derived in 3.1.2. Figure 44, Figure 45 and show the kinetic constants in function of H_2O_2 concentration.

$$[SMX]_0 = (2.568 \pm 0.061)\ AU \quad (20)$$

$$k_{SMX} = 0.003\ [H_2O_2] + 0.026;\ (r^2=0.990) \text{ until maximum 25 mM} \quad (21)$$

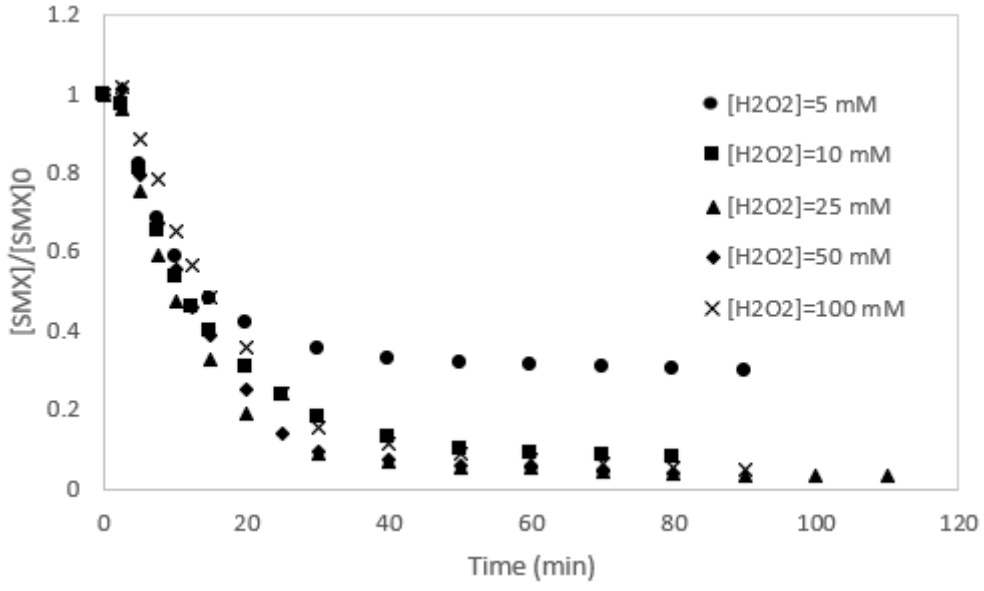

Figure 42: SMX degradation with varying [H_2O_2]

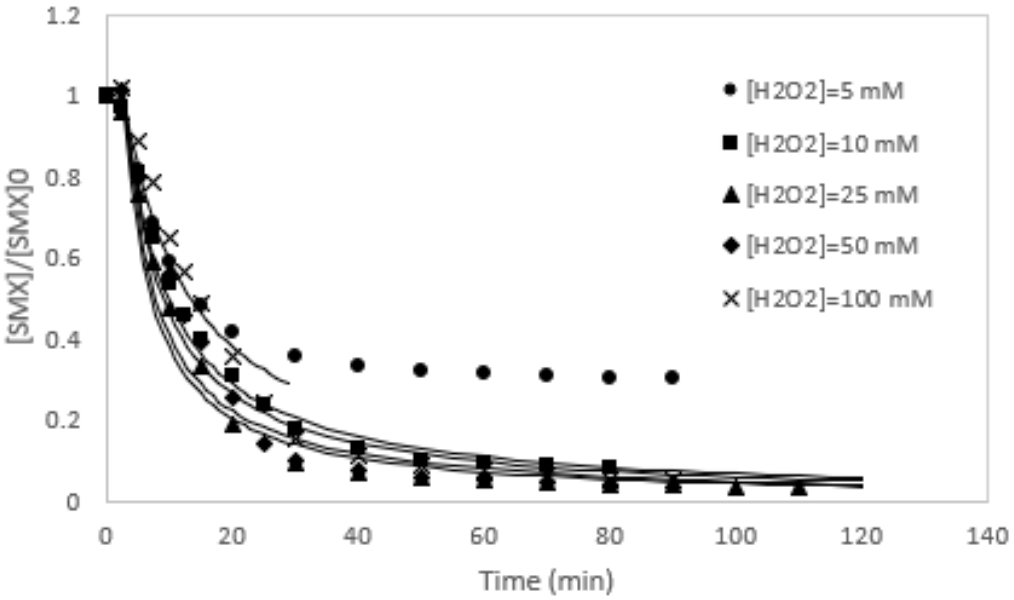

Figure 43: SMX degradation with varying [H_2O_2] and fitted second-order model

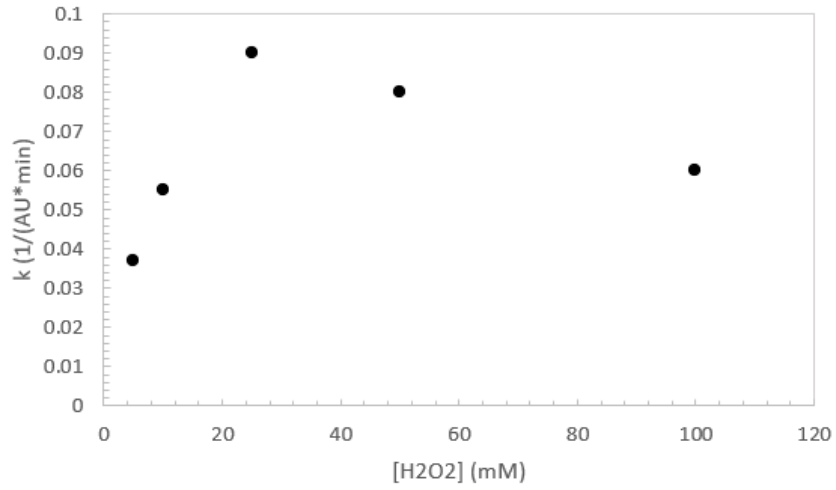

Figure 44: Kinetic constant of SMX degradation in function of [H_2O_2]

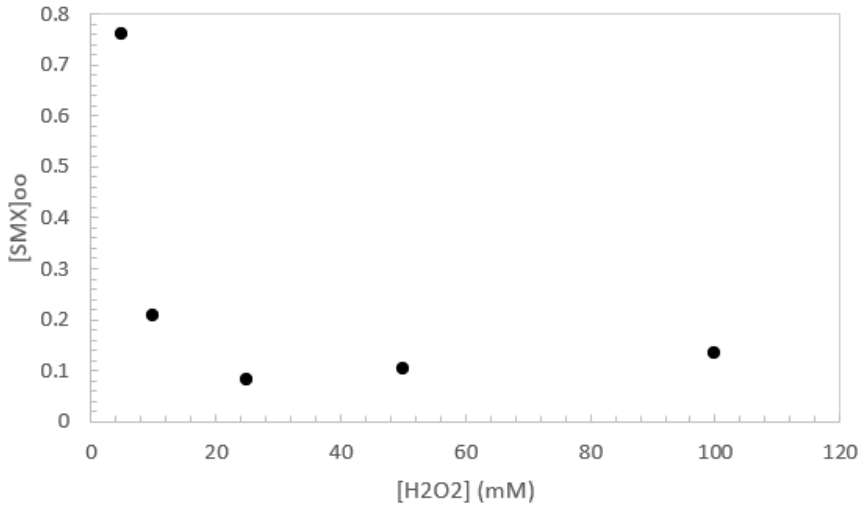

Figure 45: Steady-state measurement of SMX in function of [H_2O_2]

The kinetic constant of SMX degradation increases linearly with the H_2O_2 concentration until 25 mM, when it starts decreasing linearly. This can be attributed to the scavenging effect of excess H_2O_2, as it starts competing for OH radicals (de Freitas et al., 2013; Pera-Titus et al., 2004). The reaction of 5 mM has a significantly lower conversion of sulfamethoxazole, probably caused by insufficient H_2O_2, while this problem is avoided at 10 mM.

3.2.4. Aromaticity degradation

The aromaticity degradation is linked to the degradation of sulfamethoxazole. Thus, a second order kinetic model is proposed (Eqs. 22-24):

$$-\frac{d[A_{254}]}{dt} = k_{A_{254}} \left([A_{254}]^2 \right) \tag{22}$$

$$\frac{1}{[A_{254}]} - \frac{1}{[A_{254}]0} = -k_{A_{254}} * t \tag{23}$$

$$[A_{254}] = \frac{1}{-k_{A_{254}} * t + \frac{1}{[A_{254}]0}} \tag{24}$$

3.2.5. Aromaticity degradation: effect of Fe^{2+}

Figure 46 shows the aromaticity measurements during the reactions with varying [Fe^{2+}]. Figure 47 shows the calculated kinetic constants of the second-order model fitted to these measurements:

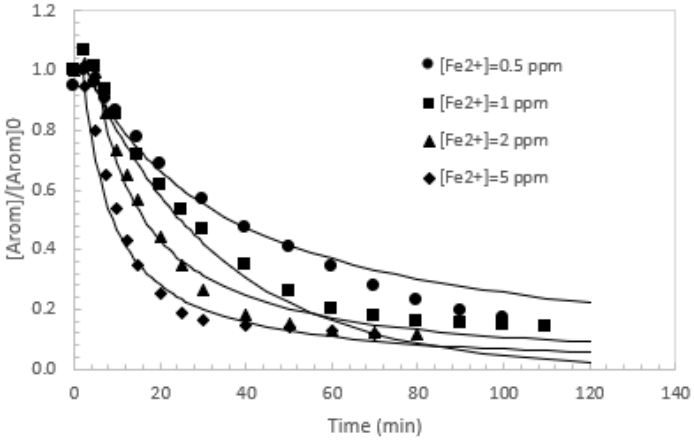

Figure 46: Aromaticity degradation for reactions with varying [Fe^{2+}] with fitted second-order model

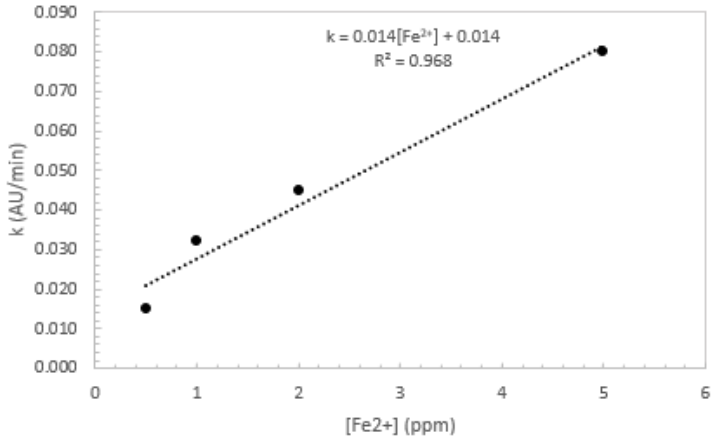

Figure 47: Kinetic constant in function of [Fe^{2+}]

The kinetic constant of aromaticity degradation increases when the dose of iron catalyst increases. This increase is linear, until higher values where a plateau would be reached (Pera-Titus et al., 2004). The average initial measurement of aromaticity was 1.892 AU with a standard deviation of 0.125 AU.

3.2.6. Aromaticity degradation: effect of H_2O_2

The aromaticity degradation during the reactions with varying H_2O_2 concentration and fitted second-order model is shown in Figure 48. The calculated kinetic constants are shown in Figure 49:

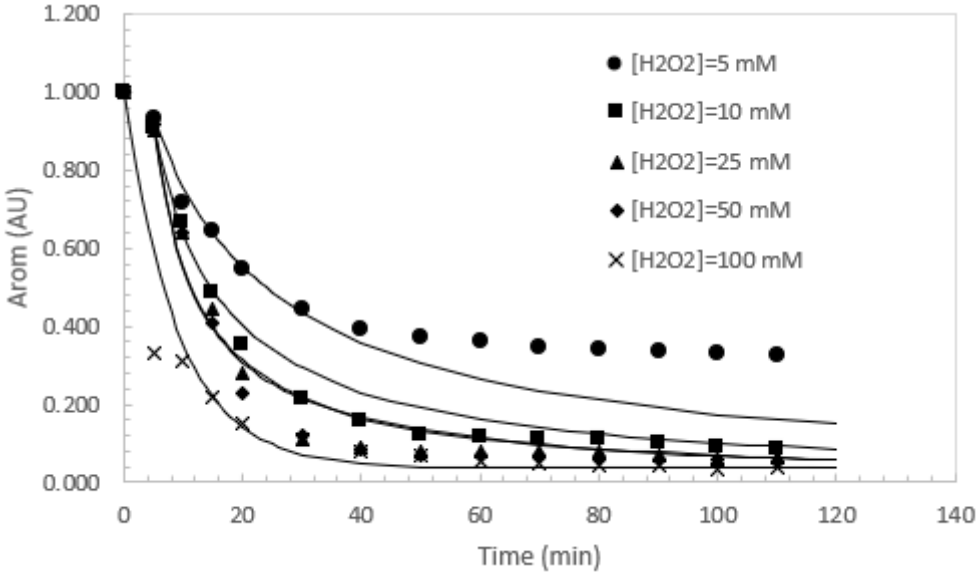

Figure 48: Aromaticity degradation for the reactions with varying [H_2O_2] and fitted second-order models

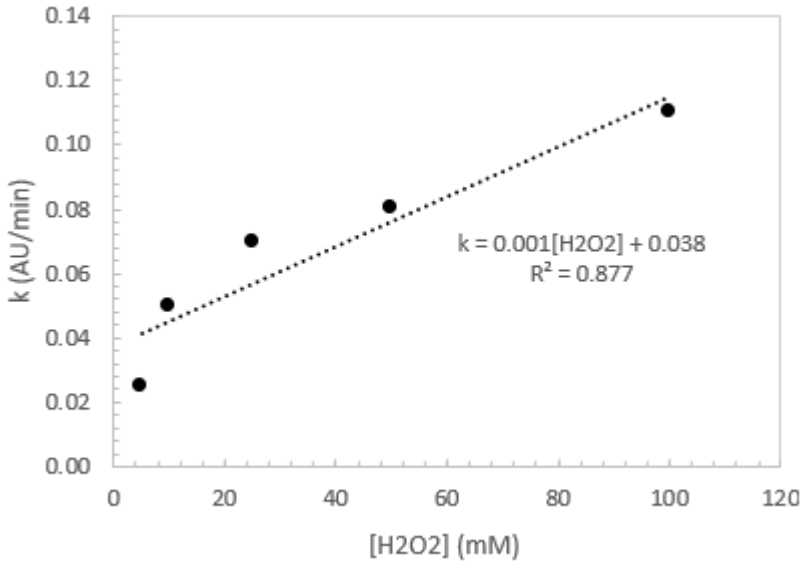

Figure 49: Second-order kinetic constant in function of [H_2O_2]

The kinetic constant of aromaticity degradation increases similarly to the kinetic constant of SMX degradation, which is with a decreasing effect at higher concentrations due to the scavenging effect of excess H_2O_2.

3.2.7. Color formation and degradation

Figure 50 shows the change in color during the reactions with varying [Fe^{2+}] and Figure 51 shows the reactions with varying [H_2O_2]. It is important to note that the line is not a fitted model, but only an extra addition for clarity. No model was created for the color and turbidity reactions due to the intricacy of making subsequent models. The conclusion is the same as for aromaticity and sulfamethoxazole: increasing the iron and hydrogen peroxide dose increases the speed of reaction and thus also the speed of color and turbidity change.

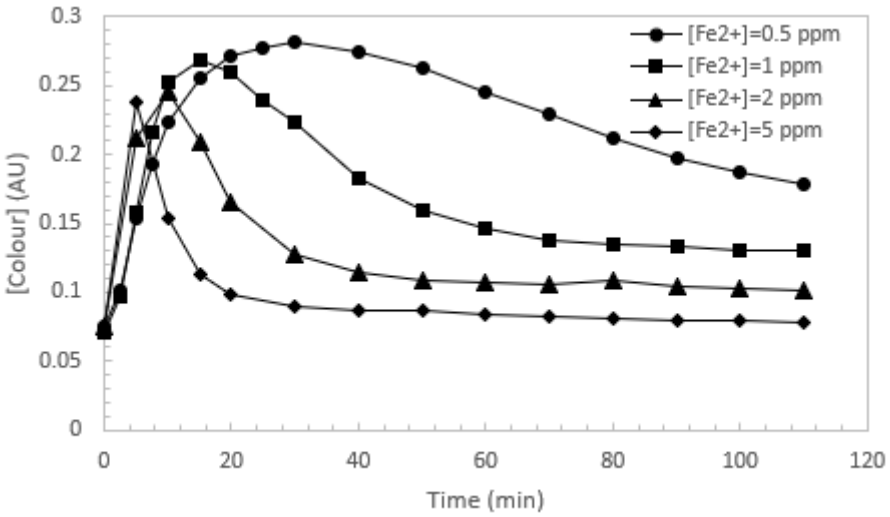

Figure 50: Color formation and degradation for the reactions with varying [Fe^{2+}]

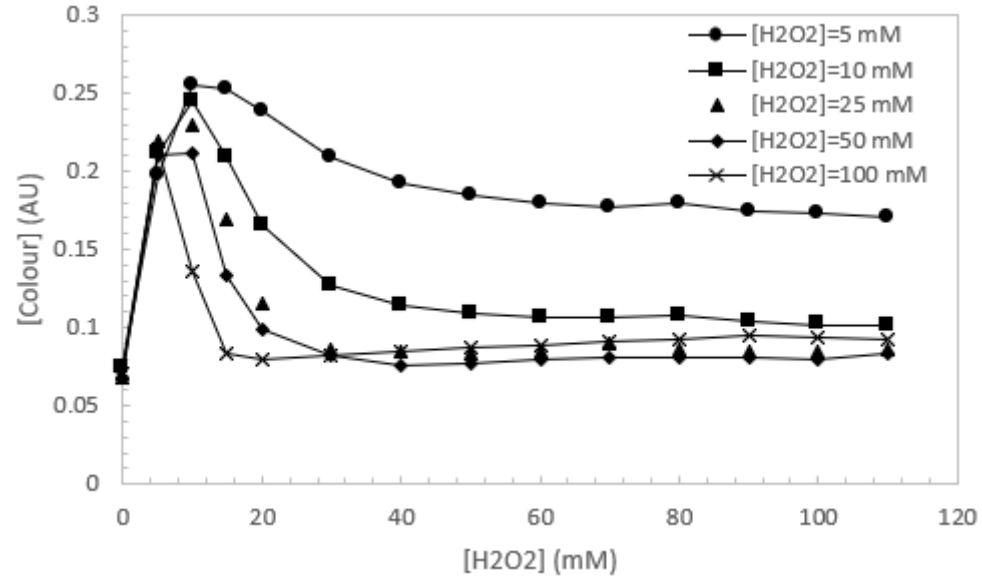

Figure 51: Color formation and degradation for the reactions with varying [H_2O_2].

Figure 50 and Figure 51 show that the formation and degradation rate are both increased by increased dose of [Fe^{2+}] and [H_2O_2]. Due to the increased efficiency of the photo-Fenton reactions, there is degradation of the color- and turbidity forming intermediates after their formation. Analysis with a separation technique such as HPLC or mass-spectroscopy could potentially identify and quantify these intermediates.

3.2.8. Turbidity formation and degradation

Figure 52 shows the change in turbidity during the reactions with varying [Fe^{2+}] and Figure 53 shows the reactions with varying [H_2O_2].

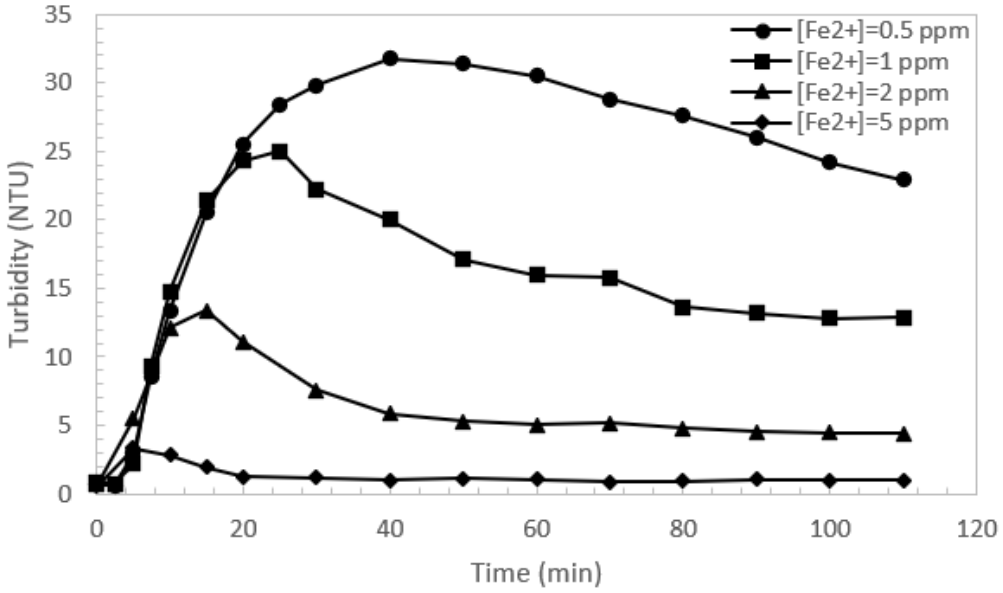

Figure 52: Turbidity formation and degradation for the reactions with varying [Fe^{2+}]

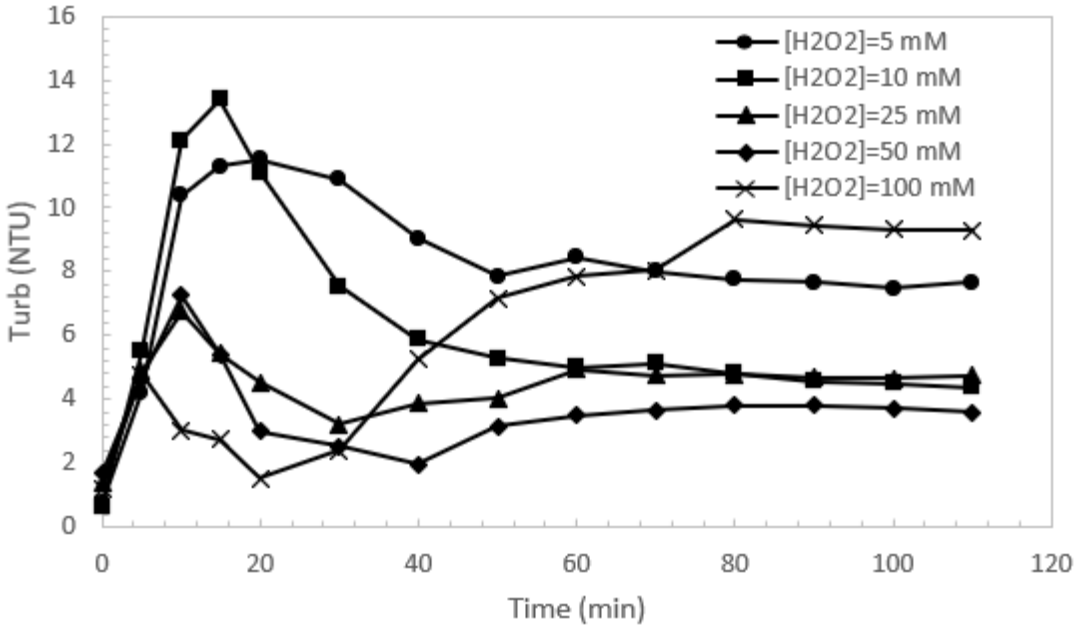

Figure 53: Turbidity formation and degradation for the reactions with varying [H_2O_2]

Both Figure 52 and Figure 53 show that the peak turbidity increases with a lower reaction rate. It seems the intermediate has more time to form before degradation occurs. Interestingly, when the H_2O_2 concentration increases above 10 mM, a second increase in turbidity occurs, indicating another intermediate that causes turbidity in the solution in the later stages of the degradation pathway.

3.3. SULFAMETHOXAZOLE DEGRADATION PATHWAY

As explained in 1.6, SMX degradation occurs through three main pathways. First, hydroxylation of the rings occurs. In a second pathway, benzene and isoxazole (colorless) ring opening occurs. Thirdly, scission of the central S-N bond followed by hydrolysis

leads to the formation of 3-amino-5-methylisoxazole (yellow) and 4-sulfonylaniline (colorless). Subsequent radical attack, leads to ring opening, resulting in the formation of carboxylic acids such as oxalic acid (colorless) and acetic acid (colorless) (Gonçalves et al., 2012; Zhong et al., 2021). It is theorized that 4-sulfonylaniline is degraded to aniline (colorless) and then to p-benzoquinone (brown) (Hu et al., 2007; Xiong et al., 2020). Hydroxylation and ring-opening reactions can occur prior to S-N bond cleavage, resulting in the formation of higher molecular weight intermediates (Trovó et al., 2009). If the oxidation reaction is completed, the organic compounds will be fully oxidized to CO_2, H_2O, NH_3 and SO_2 (Kumar et al., 2021). It is possible that p-benzoquinone, commonly found during SMX degradation in literature, is the cause of the brown color formation. Villota et al. state that, during the oxidative degradation of phenol, hydroxyquinone and muconic acid were the cause for turbidity increase (Villota et al., 2017). These compounds are very similar to the compounds described in the literature for sulfamethoxazole degradation. Further research could focus on identifying and quantifying the p-benzoquinone and muconic acid in the solution.

4. CONCLUSION

During the oxidation of SMX with UV/H_2O_2 a strong brown color is generated in the water accompanied by high turbidity formation which is a function of pH. SMX exists in positive, neutral and negative forms, because it has two ionizable amino groups. The color of water increases from pH=2.0 (light brown, 3.5 NTU) to a maximum value at pH=4.0 (dark brown, 42 NTU) when a 100% SMX is in its neutral form. Under these conditions the formation of the carboxylic acids (acetic and oxalic) is minor, because the aromatic ring opening does not occur. Nor are nitrate ions detected, indicating that species containing nitrogen atoms in their molecular structure are not mineralized. Operating at higher pH, the color decreases, obtaining at pH=12.0 light yellow water (5 NTU) when the anionic SMX dominates. Under these conditions the maximum formation of nitrate ions occur. For the UV/H_2O_2 reactions, a pseudo first-order kinetic model is proposed for the degradation of aromaticity and sulfamethoxazole and formation of color and turbidity in water. The kinetic parameters are expressed as a function of the applied pH.

The photo-Fenton reactions were characterized by a maximal intensity of color (light brown) and turbidity, followed by a decrease of both. Thus, color- and turbidity-forming intermediates were formed and subsequently degraded. Interestingly, a second peak in turbidity for the reactions with more than 25 mM H_2O_2 proves the existence of a second turbidity-forming intermediate later in the degradation pathway. For the photo-Fenton reactions, a second-order model is proposed. The kinetic parameters are expressed as a function of the Fe^{2+} concentration and H_2O_2 concentration. Generally, a faster degradation occurred by increasing Fe^{2+} or H_2O_2, but the increase diminishes at higher concentrations.

This research was focused on increasing the knowledge about the sulfamethoxazole degradation. It is theorized that p-benzoquinone is the cause for the brown color formation. Further research could focus on identifying this compound and other intermediates through separation and detection techniques such as HPLC and mass-spectrometry.

References

Alaee, M., & Wenning, R. J. (2002). The significance of brominated flame retardants in the environment: current understanding, issues and challenges. *Chemosphere*, *46*(5), 579–582. https://doi.org/10.1016/S0045-6535(01)00224-7

Bahlai, C. A., Xue, Y., McCreary, C. M., Schaafsma, A. W., & Hallett, R. H. (2010). Choosing organic pesticides over synthetic pesticides may not effectively mitigate environmental risk in soybeans. *PLoS ONE*, *5*(6). https://doi.org/10.1371/JOURNAL.PONE.0011250

Baird, R. B., & Bridgewater, L. (2017). Standard methods for the Examination of Water and Wastewater. In A. D. Eaton, L. S. Clesceri, & A. E. Greenberg (Eds.), *American Public Health Association, American Water Works* (Vol. 23). APHA (American Public Health Association).

Borowska, E., Felis, E., & Miksch, K. (2015). Degradation of sulfamethoxazole using UV and UV/H2O2 processes. *Journal of Advanced Oxidation Technologies*, *18*(1), 69–77. https://doi.org/10.1515/JAOTS-2015-0109/MACHINEREADABLECITATION/RIS

Boule, P., Guyon, C., & Lemaire, J. (1984). Vi. Direct Phototransformation Of Chlorophenols And Interactions With Phenol On Uv Exposure In Aqueous Solution. *Toxicological & Environmental Chemistry*, *7*(2), 97–110. https://doi.org/10.1080/02772248409357020

Boutiti, A., Zouaghi, R., Bendjabeur, S. E., Guittonneau, S., & Sehili, T. (2017). Photodegradation of 1-hexyl-3-methylimidazolium by UV/H2O2 and UV/TiO2: Influence of pH and chloride. *Journal of Photochemistry and Photobiology A: Chemistry*, *336*, 164–169. https://doi.org/10.1016/J.JPHOTOCHEM.2016.12.030

Braeken, L. (2021). *Ecologie en capita selecta waterbehandeling [cursus]*. Diepenbeek: Gezamenlijke opleiding Industriële Ingenieurswetenschappen UHasselt & KU Leuven.

Buxton, G. v., Greenstock, C. L., Helman, W. P., & Ross, A. B. (2009). Critical Review of rate constants for reactions of hydrated electrons, hydrogen atoms and hydroxyl radicals (·OH/·O− in Aqueous Solution. *Journal of Physical and Chemical Reference Data*, *17*(2), 513. https://doi.org/10.1063/1.555805

C. Underwood, J., W. Harvey, R., W. Metge, D., A. Repert, D., K. Baumgartner, L., L. Smith, R., M. Roane, T., & B. Barber, L. (2011). Effects of the Antimicrobial Sulfamethoxazole on Groundwater Bacterial Enrichment. *Environmental Science & Technology*, *45*(7), 3096–3101. https://doi.org/10.1021/es103605e

Carrizales, S. (2020). *Single and ternary removal of sulfonamidas from water using activated carbon* [PhD]. Universidad Autónoma de San Luis Potosí.

Chamarro, E., Marco, A., & Esplugas, S. (2001). Use of Fenton reagent to improve organic chemical biodegradability. *Water Research*, *35*(4), 1047–1051. https://doi.org/10.1016/S0043-1354(00)00342-0

Choquet-Kastylevsky, G., Vial, T., & Descotes, J. (2002). Allergic Adverse Reactions to Sulfonamides. *Current Allergy and Asthma Reports*, *2*, 16–25.

Daughton, C. G. (2004). Non-regulated water contaminants: emerging research. *Environmental Impact Assessment Review*, *24*(7–8), 711–732. https://doi.org/10.1016/J.EIAR.2004.06.003

de Freitas, A. M., Sirtori, C., Lenz, C. A., & Zamora, P. G. P. (2013). Microcystin-LR degradation by solar photo-Fenton, UV-A/photo-Fenton and UV-C/H2O2: a comparative study. *Photochemical & Photobiological Sciences 2013 12:4*, *12*(4), 696–702. https://doi.org/10.1039/C2PP25233C

der Beek, T. A., Weber, F.-A., Bergmann, A., Hickmann, S., Ebert, I., Hein, A., & Küsterz, A. (2015). PHARMACEUTICALS IN THE ENVIRONMENT-GLOBAL OCCURRENCES AND PERSPECTIVES. *Environmental Toxicology and Chemistry*, *35*(4), 823–835. https://doi.org/10.1002/etc.3339

Dieleman, J. L., Squires, E., Bui, A. L., Campbell, M., Chapin, A., Hamavid, H., Horst, C., Li, Z., Matyasz, T., Reynolds, A., Sadat, N., Schneider, M. T., & Murray, C. J. L. (2017). Factors Associated With Increases in US Health Care Spending, 1996-2013. *JAMA*, *318*(17), 1668–1678. https://doi.org/10.1001/JAMA.2017.15927

Diniz, M. S., Maurício, R., Petrovic, M., de Alda, M. J. L., Amaral, L., Peres, I., Barceló, D., & Santana, F. (2010). Assessing the estrogenic potency in a Portuguese wastewater treatment plant using an integrated approach. *Journal of Environmental Sciences*, *22*(10), 1613–1622. https://doi.org/10.1016/S1001-0742(09)60297-7

European Union. (2008). *On environmental quality standards in the field of water policy*. https://eur-lex.europa.eu/legal-content/EN/TXT/?uri=celex%3A32008L0105

European Union. (2012). *A Blueprint to Safeguard Europe's Water Resources*. https://eur-lex.europa.eu/legal-content/EN/TXT/?uri=COM:2012:0673:FIN

FDA. (n.d.). *Bactrim USPI*.

Fent, K., Weston, A. A., & Caminada, D. (2006). Ecotoxicology of human pharmaceuticals. *Aquatic Toxicology*, *76*(2), 122–159. https://doi.org/10.1016/J.AQUATOX.2005.09.009

Gao, J., Huang, J., Chen, W., Wang, B., Wang, Y., Deng, S., & Yu, G. (2016). Fate and removal of typical pharmaceutical and personal care products in a wastewater treatment plant from Beijing: a mass balance study. *Frontiers of Environmental Science & Engineering 2016 10:3*, *10*(3), 491–501. https://doi.org/10.1007/S11783-016-0837-Y

García, J. (2007). *Combination of Advanced Oxidation Processes and Biological Treatments for Commercial Reactive Azo Dyes Removal* [PhD]. Universitat Autònoma de Barcelona.

Glüge, J., Schinkel, L., Hungerbühler, K., Cariou, R., & Bogdal, C. (2018). Environmental Risks of Medium-Chain Chlorinated Paraffins (MCCPs): A Review. *Environmental Science and Technology*, *52*(12), 6743–6760. https://doi.org/10.1021/acs.est.7b06459

Gonçalves, A. G., órfão, J. J. M., & Pereira, M. F. R. (2012). Catalytic ozonation of sulphamethoxazole in the presence of carbon materials: Catalytic performance and reaction pathways. *Journal of Hazardous Materials*, *239–240*, 167–174. https://doi.org/10.1016/j.jhazmat.2012.08.057

Halling-Sorensen, B., Nielsen, S. N., Lanzky, P. F., Ingerslev, F., Liitzhofl, H. C. H., & Jorgensen, S. E. (1998). Occurrence, Fate and Effects of Pharmaceutical Substances in the Environment-A Review. In *Chemosphere* (Vol. 36, Issue 2).

Hollman, J., Dominic, J. A., & Achari, G. (2020). Degradation of pharmaceutical mixtures in aqueous solutions using UV/peracetic acid process: Kinetics, degradation pathways and comparison with UV/H2O2. *Chemosphere*, *248*, 125911. https://doi.org/10.1016/J.CHEMOSPHERE.2020.125911

Hu, L., Flanders, P. M., Miller, P. L., & Strathmann, T. J. (2007). Oxidation of sulfamethoxazole and related antimicrobial agents by TiO2 photocatalysis. *Water Research*, *41*(12), 2612–2626. https://doi.org/10.1016/j.watres.2007.02.026

Jaeger, J. W., Carlson, I. H., & Porter, W. P. (1999). Endocrine, immune, and behavioral effects of aldicarb (carbamate), atrazine (triazine) and nitrate (fertilizer) mixtures at groundwater concentrations. *Toxicology and Industrial Health*, *15*(2), 133–151. https://doi.org/10.1177/074823379901500111

Kehrer, J. P., Robertson, J. D., & Smith, C. v. (2010). Free Radicals and Reactive Oxygen Species. *Comprehensive Toxicology: Second Edition*, *1–14*, 277–307. https://doi.org/10.1016/B978-0-08-046884-6.00114-7

Kim, Y. R., Harden, F. A., Toms, L. M. L., & Norman, R. E. (2014). Health consequences of exposure to brominated flame retardants: A systematic review. *Chemosphere*, *106*, 1–19. https://doi.org/10.1016/J.CHEMOSPHERE.2013.12.064

Kmmerer, K. (2010). Pharmaceuticals in the environment. *Annual Review of Environment and Resources*, *35*, 57–75. https://doi.org/10.1146/annurev-environ-052809-161223

Kumar, A., Sharma, S. K., Sharma, G., Guo, C., Vo, D. V. N., Iqbal, J., Naushad, M., & Stadler, F. J. (2021). Silicate glass matrix@Cu2O/Cu2V2O7 p-n heterojunction for enhanced visible light photo-degradation of sulfamethoxazole: High charge separation and interfacial transfer. *Journal of Hazardous Materials*, *402*, 123790. https://doi.org/10.1016/J.JHAZMAT.2020.123790

Kurrer, C. (2021, October). *Fact Sheets on the European Union: Water protection and management*. https://www.europarl.europa.eu/factsheets/en/sheet/74/water-protection-and-management

Kurup, L. (2012). Evaluation of the adsorption capacity of alkali-treated waste materials for the adsorption of sulphamethoxazole. *Water Science and Technology : A Journal of the International Association on Water Pollution Research*, *65*(9), 1531–1539. https://doi.org/10.2166/WST.2012.017

Kuster, M., López de Alda, M. J., Hernando, M. D., Petrovic, M., Martín-Alonso, J., & Barceló, D. (2008). Analysis and occurrence of pharmaceuticals, estrogens, progestogens and polar pesticides in sewage treatment plant effluents, river water and drinking water in the Llobregat river basin (Barcelona, Spain). *Journal of Hydrology*, *358*(1–2), 112–123. https://doi.org/10.1016/j.jhydrol.2008.05.030

Legrini, O., Oliveros, E., & M. Braun, A. (2002). Photochemical processes for water treatment. *Chemical Reviews*, *93*(2), 671–698. https://doi.org/10.1021/cr00018a003

Lester, Y., Avisar, D., & Mamane, H. (2010). Photodegradation of the antibiotic sulphamethoxazole in water with UV/H2O2 advanced oxidation process. *Environmental Technology*, *31*(2), 175–183. https://doi.org/10.1080/09593330903414238

Liu, Y., Zhu, K., Su, M., Zhu, H., Lu, J., Wang, Y., Dong, J., Qin, H., Wang, Y., & Zhang, Y. (2019). Influence of solution pH on degradation of atrazine during UV and UV/H2O2 oxidation: kinetics,

mechanism, and degradation pathways. *RSC Advances*, *9*(61), 35847–35861. https://doi.org/10.1039/C9RA05747A

Martínez-Costa, J. I., Rivera-Utrilla, J., Leyva-Ramos, R., Sánchez-Polo, M., Velo-Gala, I., & Mota, A. J. (2018). Individual and simultaneous degradation of the antibiotics sulfamethoxazole and trimethoprim in aqueous solutions by Fenton, Fenton-like and photo-Fenton processes using solar and UV radiations. *Journal of Photochemistry and Photobiology A: Chemistry*, *360*, 95–108. https://doi.org/10.1016/J.JPHOTOCHEM.2018.04.014

Mijangos, F., Varona, F., & Villota, N. (2006). Changes in solution color during phenol oxidation by fenton reagent. *Environmental Science and Technology*, *40*(17), 5538–5543. https://doi.org/10.1021/ES060866Q/SUPPL_FILE/ES060866QSI20060619_063730.PDF

Moran, S. (2018). *An Applied Guide to Water and Effluent Treatment Plant Design* (1st ed.). Amsterdam: Elsevier Science Publishing Co Inc.

Murray, K. E., Thomas, S. M., & Bodour, A. A. (2010). Prioritizing research for trace pollutants and emerging contaminants in the freshwater environment. *Environmental Pollution*, *158*(12), 3462–3471. https://doi.org/10.1016/J.ENVPOL.2010.08.009

Naraginti, S., Li, Y., & Puma, G. L. (2018). Photocatalytic mineralization and degradation kinetics of sulphamethoxazole and reactive red 194 over silver-zirconium co-doped titanium dioxide: Reaction mechanisms and phytotoxicity assessment. *Ecotoxicology and Environmental Safety*, *159*, 301–309. https://doi.org/10.1016/J.ECOENV.2018.04.062

Nghiem, L. D., Espendiller, C., & Braun, G. (2008). Influence of organic and colloidal fouling on the removal of sulphamethoxazole by nanofiltration membranes. *Water Science and Technology : A Journal of the International Association on Water Pollution Research*, *58*(1), 163–169. https://doi.org/10.2166/WST.2008.647

Oberg, O., & Warman, K. (2002). Distribution and levels of brominated flame retardants in sewage sludge. *Chemosphere*, *48*, 805–809. https://doi.org/https://doi.org/10.1016/S0045-6535(02)00113-3

Pandis, P. K., Kalogirou, C., Kanellou, E., Vaitsis, C., Savvidou, M. G., Sourkouni, G., Zorpas, A. A., & Argirusis, C. (2022). Key Points of Advanced Oxidation Processes (AOPs) for Wastewater, Organic Pollutants and Pharmaceutical Waste Treatment: A Mini Review. In *ChemEngineering* (Vol. 6, Issue 1). MDPI. https://doi.org/10.3390/chemengineering6010008

Pera-Titus, M., García-Molina, V., Baños, M. A., Giménez, J., & Esplugas, S. (2004). Degradation of chlorophenols by means of advanced oxidation processes: A general review. *Applied Catalysis B: Environmental*, *47*(4), 219–256. https://doi.org/10.1016/j.apcatb.2003.09.010

Petrovic, M., de Alda, M. J. L., Diaz-Cruz, S., Postigo, C., Radjenovic, J., Gros, M., & Barcelo, D. (2009). Fate and removal of pharmaceuticals and illicit drugs in conventional and membrane bioreactor wastewater treatment plants and by riverbank filtration. In *Philosophical Transactions of the Royal Society A: Mathematical, Physical and Engineering Sciences* (Vol. 367, Issue 1904, pp. 3979–4003). Royal Society. https://doi.org/10.1098/rsta.2009.0105

Petrović, M., Gonzalez, S., & Barceló, D. (2003). Analysis and removal of emerging contaminants in wastewater and drinking water. *TrAC - Trends in Analytical Chemistry*, *22*(10), 685–696. https://doi.org/10.1016/S0165-9936(03)01105-1

Qiang, Z., & Adams, C. (2004). Potentiometric determination of acid dissociation constants (pKa) for human and veterinary antibiotics. *Water Research*, *38*(12), 2874–2890. https://doi.org/10.1016/J.WATRES.2004.03.017

Rawn, D. F. K., Dufresne, G., Clément, G., Fraser, W. D., & Arbuckle, T. E. (2022). Perfluorinated alkyl substances in Canadian human milk as part of the Maternal-Infant Research on Environmental Chemicals (MIREC) study. *Science of The Total Environment*, *831*, 154888. https://doi.org/10.1016/J.SCITOTENV.2022.154888

Rosal, R., Rodríguez, A., Perdigón-Melón, J. A., Petre, A., García-Calvo, E., Gómez, M. J., Agüera, A., & Fernández-Alba, A. R. (2010). Occurrence of emerging pollutants in urban wastewater and their removal through biological treatment followed by ozonation. *Water Research*, *44*(2), 578–588. https://doi.org/10.1016/J.WATRES.2009.07.004

Rossberg, M., Lendle, W., Pfleiderer, G., Dreher, E.-L., Langer, E., Rassaerts, H., Kleinschmidt, P., Cook, R., Beck, U., & Beutel, K. K. (2006). Chlorinated Hydrocarbons. *Ullmann's Encyclopedia of Industrial Chemistry*. https://doi.org/https://doi.org/10.1002/14356007.a06_233.pub2

Roth, L., Adler, M., Jain, T., & Bempong, D. (2018). Monographs for medicines on who's model list of essential medicines. *Bulletin of the World Health Organization*, *96*(6), 378–385. https://doi.org/10.2471/BLT.17.205807

Santos-Juanes, L., Sánchez, J. L. G., López, J. L. C., Oller, I., Malato, S., & Sánchez Pérez, J. A. (2011). Dissolved oxygen concentration: A key parameter in monitoring the photo-Fenton process. *Applied Catalysis B: Environmental*, *104*(3–4), 316–323. https://doi.org/10.1016/J.APCATB.2011.03.013

Sherman, P. O., & Smith, S. (1971). *BLOCK AND GRAFT COPOLYMERS CONTAINING WATER-SOLWATABLE POLAR GROUPS AND FLUOROALEPHATIC GROUPS* (Patent No. US3574791A).

Shoaib Khan, H. M., & Sajid Ur Rehman, M. (2012). Influence of pH and Temperature on Stability of Sulfamethoxazole Alone and in Combination with Trimethoprim (Co Trimoxazole). *Asian Journal of Chemistry*, *24*(4), 1851–1854. https://www.researchgate.net/publication/294659867

Steenland, K., Fletcher, T., & Savitz, D. A. (2010). Epidemiologic Evidence on the Health Effects of Perfluorooctanoic Acid (PFOA). *Environmental Health Perspectives*, *118*(8), 1100–1108. https://doi.org/10.1289/ehp.0901827

Tev, S., Morgan, E. N., Cu, C. N., & Ngham, N. (2011). Population Aging and the Determinants of Healthcare Expenditures: The Case of Hospital, Medical and Pharmaceutical Care in British Columbia, 1996 to 2006. *Healthcare Policy*, *7*(1), 68. /pmc/articles/PMC3167569/

Trovó, A. G., Nogueira, R. F. P., Agüera, A., Fernandez-Alba, A. R., Sirtori, C., & Malato, S. (2009). Degradation of sulfamethoxazole in water by solar photo-Fenton. Chemical and toxicological evaluation. *Water Research*, *43*(16), 3922–3931. https://doi.org/10.1016/J.WATRES.2009.04.006

United Stated Environmental Protection Agency (EPA). (n.d.). *Contaminants of Emerging Concern including Pharmaceuticals and Personal Care Products*.

Villota, N., Coralli, I., & Lomas, J. M. (2021). Changes of dissolved oxygen in aqueous solutions of caffeine oxidized by photo-Fenton reagent. *Environmental Technology*, *42*(4), 609–617. https://doi.org/10.1080/09593330.2019.1639830

Villota, N., Lomas, J. M., & Camarero, L. M. (2016). Study of the paracetamol degradation pathway that generates color and turbidity in oxidized wastewaters by photo-Fenton technology. *Journal of Photochemistry and Photobiology A: Chemistry*, *329*, 113–119. https://doi.org/10.1016/j.jphotochem.2016.06.024

Villota, N., Lomas, J. M., & Camarero, L. M. (2017). Effect of ultrasonic waves on the water turbidity during the oxidation of phenol. Formation of (hydro)peroxo complexes. *Ultrasonics Sonochemistry*, *39*, 439–445. https://doi.org/10.1016/J.ULTSONCH.2017.05.024

Walling, C. (2002). Fenton's reagent revisited. *Accounts of Chemical Research*, *8*(4), 125–131. https://doi.org/10.1021/ar50088a003

Wang, J., & Wang, S. (2016). Removal of pharmaceuticals and personal care products (PPCPs) from wastewater: A review. *Journal of Environmental Management*, *182*, 620–640. https://doi.org/10.1016/J.JENVMAN.2016.07.049

Wang, J., & Wang, S. (2018). Microbial degradation of sulfamethoxazole in the environment. *Applied Microbiology and Biotechnology*, *102*(8), 3573–3582. https://doi.org/10.1007/S00253-018-8845-4/FIGURES/1

Wang, X., Shi, X., Zheng, S., Zhang, Q., Peng, J., & Wu, K. (2022). Perfluorooctane Sulfonic Acid (Pfos) Exposures Interfere Behaviors and Transcriptions of Genes on Nervous and Muscle System in Zebrafish Embryos. *SSRN Electronic Journal*. https://doi.org/10.2139/SSRN.4081350

Watanabe, I. (1987). POLYBROMINATED BIPHENYL ETHERS IN MARINE FISH, SHELLFISH AND RIVER AND MARINE SEDIMENTS IN JAPAN. *Chemosphere*, *16*(10–12), 2389–2396.

Weishaar, J. L., Aiken, G. R., Bergamaschi, B. A., Fram, M. S., Fujii, R., & Mopper, K. (2003). Evaluation of specific ultraviolet absorbance as an indicator of the chemical composition and reactivity of dissolved organic carbon. *Environmental Science and Technology*, *37*(20), 4702–4708. https://doi.org/10.1021/ES030360X/ASSET/IMAGES/LARGE/ES030360XF00005.JPEG

Wu, S. H., Chu, H. Q., Dong, B. Z., Zhou, J. R., & Huang, Y. (2010). Removal of sulfamethoxazole by nanofiltration membrane. *Journal of Zhejiang University-SCIENCE A 2010 11:11*, *11*(11), 868–878. https://doi.org/10.1631/JZUS.A0900606

Xiong, Q., Liu, Y. S., Hu, L. X., Shi, Z. Q., Cai, W. W., He, L. Y., & Ying, G. G. (2020). Co-metabolism of sulfamethoxazole by a freshwater microalga Chlorella pyrenoidosa. *Water Research*, *175*, 115656. https://doi.org/10.1016/J.WATRES.2020.115656

Yang, Y., Lu, X., Jiang, J., Ma, J., Liu, G., Cao, Y., Liu, W., Li, J., Pang, S., Kong, X., & Luo, C. (2017). Degradation of sulfamethoxazole by UV, UV/H2O2 and UV/persulfate (PDS): Formation of oxidation products and effect of bicarbonate. *Water Research*, *118*, 196–207. https://doi.org/10.1016/J.WATRES.2017.03.054

Younes, M., & Galal-Gorchev, H. (2000). Pesticides in drinking water—A case study. *Food and Chemical Toxicology*, *38*(SUPPL.1), S87–S90. https://doi.org/10.1016/S0278-6915(99)00132-5

Zhang, R., Yang, Y., Huang, C. H., Zhao, L., & Sun, P. (2016). Kinetics and modeling of sulfonamide antibiotic degradation in wastewater and human urine by UV/H2O2 and UV/PDS. *Water Research*, *103*, 283–292. https://doi.org/10.1016/J.WATRES.2016.07.037

Zhang, Y., Mustieles, V., Sun, Y., Oulhote, Y., Wang, Y.-X., & Messerlian, C. (2022). Association between serum per- and polyfluoroalkyl substances concentrations and common cold among children and adolescents in the United States. *Environment International*, *164*, 107239. https://doi.org/10.1016/J.ENVINT.2022.107239

Zhong, J., Yang, B., Gao, F. Z., Xiong, Q., Feng, Y., Li, Y., Zhang, J. N., & Ying, G. G. (2021). Performance and mechanism in degradation of typical antibiotics and antibiotic resistance genes by magnetic resin-mediated UV-Fenton process. *Ecotoxicology and Environmental Safety*, *227*, 112908. https://doi.org/10.1016/J.ECOENV.2021.112908

Zhou, L. J., Ying, G. G., Liu, S., Zhao, J. L., Yang, B., Chen, Z. F., & Lai, H. J. (2013). Occurrence and fate of eleven classes of antibiotics in two typical wastewater treatment plants in South China. *Science of The Total Environment*, *452–453*, 365–376. https://doi.org/10.1016/J.SCITOTENV.2013.03.010

Zhou, Z., Zhen, J., Karpowich, N. K., Goetz, R. M., Law, C. J., A Reith, M. E., & Wang, D.-N. (2007). LeuT-desipramine structure suggests how antidepressants inhibit human neurotransmitter transporters. *Science*, *317*(5843), 1390–1393. https://doi.org/10.1126/science.1147614

Zhu, G., Sun, Q., Wang, C., Yang, Z., & Xue, Q. (2019). Removal of Sulfamethoxazole, Sulfathiazole and Sulfamethazine in their Mixed Solution by UV/H2O2 Process. *International Journal of Environmental Research and Public Health 2019, Vol. 16, Page 1797*, *16*(10), 1797. https://doi.org/10.3390/IJERPH16101797